Eng. Sci., 2021, **16**, 26–46

Engineered Science

DOI: https://dx.doi.org/10.30919/es8d553

# Influence of Temperature on Mechanical Properties and Machining of Fibre Reinforced Polymer Composites: A Review

S. M. Shahabaz,[1] Sathyashankara Sharma,[1] Nagaraja Shetty,[1,*] S. Divakara Shetty[2] and M. C. Gowrishankar[1]

## Abstract

Fiber-reinforced polymer (FRP) composites are revolutionizing the global manufacturing sectors due to their superior material properties. FRP's mechanical performance at various temperatures is gaining attention in aerospace, marine, and civil industries. These composites are examined for various mechanical properties at room temperature or below the glass transition temperature of the polymer matrix. The challenge exists at times of actual service conditions, as the components made of these composites are exposed to different temperature environments. At various machining operations, thermal stresses are generated due to the increase in cutting temperature between the tool-workpiece interface, leading to the catastrophic failure of the component when subjected to prolonged service time. This review comprehensively discusses the prominence of low and high temperature affecting the mechanical performance and various machining conditions of FRP composites. More than 80 research articles have been analyzed and summarized on temperature outcomes of tensile, flexural, and compressive properties. The influence of cutting temperature on different machining operations such as orthogonal cutting, milling, edge trimming, and drilling on surface characteristics and tool wear at various temperatures has also been discussed. In addition, tensile properties numerical predictive models for FRP composites exposed to elevated temperatures are presented, providing up-to-date progress.

*Keywords:* FRP composites; Mechanical properties; Thermal treatment; Machining; Cutting temperature.
Received: 15 September 2021; Accepted: 19 October 2021.
Article type: Review article.

## 1. Introduction

Most promising material to be globally used in aerospace,[1] automotive,[2] naval industry,[3] and civil structures,[4] replacing the historic metallic materials are fibre reinforced polymer (FRP) composites. FRP composites exhibit superior properties such as high strength to weight ratio, high stiffness, excellent endurance limit, improved fatigue resistance, and high corrosion resistance over conventional metallic materials.[5] Because of these unique properties, they are extensively used in aircraft components such as fuselage, outer flaps, spoilers in an automobile, and high, low-temperature applications in high-density electronic systems, satellite components.[6,7] In addition to these, FRP's are used for strengthening/retrofitting of existing or damaged concrete structural members.

When exposed to fire and high temperatures, FRP composites produced from the thermosetting matrix, mechanical properties deteriorate starkly, as the resin softens and decomposes with the temperature exceeding glass transition temperature. Due to the lower rate of flame retardancy, various polymer composites cannot be used in some specific applications.[8] Although carbon fibre reinforced polymer (CFRP) composites are advantageous in multiple applications. Their incapability of continuous heat dissipation due to the lower thermal conductivity of polymer matrix limits their use in thermal applications.[9–12] In various structures, mechanical degradation occurs when exposed to temperature variations over a continuous period.[13] Due to these temperature variations, the overall properties of composites are affected in actual service conditions.[14] For the above structural applications, the ideal requirements of high thermal conductivity, low thermal expansion, and in-depth knowledge of the temperature behavior of composites are necessary.[15,16] Hence, a thorough understanding of the temperature variation behavior of FRP composites is highly essential for the in-service condition of assessing mechanical behavior and various modes of failure in such safety-critical applications.

[1] *Department of Mechanical and Manufacturing Engineering, Manipal Institute of Technology, Manipal Academy of Higher Education, Manipal- 576 104, India.*
[2] *Mangalore Institute of Technology & Engineering (MITE), Badaga Mijar, Near Moodabidri- 574 225, Mangalore, India.*
**E-mail:* nagaraj.shetty@manipal.edu (N. Shetty)

Various types of stresses are imperiled to composites during fabrication, storage and machining operations. The stresses generated are of constant load or dynamic load. In dynamic loading, multiaxial stresses are generated where the design aspects and failure criteria based on the uniaxial stresses are not applicable.[17,18] In addition to the above stresses, residual thermal stresses are also developed at the fibre/matrix interface region due to thermal mismatch, as the temperature drops below the fabrication temperature.[19] The factors for thermal stresses in FRP composites are lack of adhesion between reinforcement and matrix, the volume fraction of reinforcement, and the amount of voids present.[20] Also, polymer matrix are highly temperature-dependent. As their temperature increases, their modulus falls several orders lower, and with decreasing temperature, they display brittle nature behavior, allowing crack propagation initiation in composites.[21] Rapid changes in the service environment affect these composites, altering the mechanical performance at different loading conditions.

There is a limited study in the literature displaying the effect of temperature and thermal cycling effects on FRP composites when exposed under various loading conditions. The variables affecting the dominance of FRP's final products are different manufacturing techniques implemented, types and configurations of fibres, and different kinds of resins applied. Moreover, based on various FRP applications, composite structures' structural performance and machining quality at different temperatures are distinguished. Concerning the above statement authors, Micelli and Nanni[22] called attention to that each component made of FRP composites has specified constituents and production methods; therefore, the ends drawn for one material are not pertinent to others. However, more infallible results can be presented when there are many datasets from numerous studies for comparison.

This paper comprehensively reviews the experimental and numerical findings, providing a foundation for exploring the behavior of FRP composites at various elevated temperatures. Initially, the damage mechanism and various mechanical properties (*i.e.*, tensile, flexural, and compressive) exposed to elevated temperatures are briefly discussed. Also, the numerical models established for relating temperature with tensile properties are also explained. Later, various conventional machining operations performed with varying conditions of temperature and their effects on thermal-induced damages are summarized for the readers. In the final section, suggestions for future work are provided, and the conclusions are drawn.

## 2. Degradation mechanism of FRP composites

In civil structures, FRP composites are implemented in various shapes (*i.e.*, I-shaped channels, tubes, reinforcing bars, sheets, strips).[23–26] Structures made of FRP's are a matter of concern under aggressive environment and cementitious environment as they are prone to premature debonding failure raising worries about the durability of the structures.[22,27]

FRP composites exposed in the temperature range of 65 to 120 °C are considered as glass transition temperature ($T_g$) where the matrix (resin) changes its state from a glassy to a rubbery state.[28] Besides this FRP's exposure to higher temperatures (*i.e.* 300 to 500 °C) causes their natural framework to deteriorate, producing heat, smoke, and ash with harmful volatiles.[29] This higher temperature is called resin decomposition temperature ($T_d$), causing chemical bonds and modular chains between resin and fibres to break.[30–33] Based on the study of Wang *et al*.[34] reinforcement loses half of its strength at critical temperature (*i.e.* 50% loss in mechanical strength is noted). Fig. 1 represents the change in the mechanical property of FRP's with temperature. In Fig. 1, initially, there is no change in mechanical property from initial room temperature until softening temperature ($T_s$) is reached. With increasing temperature (*i.e.* rising $T_s$), the mechanical property extends to a residual value ($P_{residual}$) where the composite reaches the melting temperature ($T_m$). The region beyond the ($T_s$) is termed as glass transition range, as the resin matrix changes its state from brittle to rubbery state.[35]

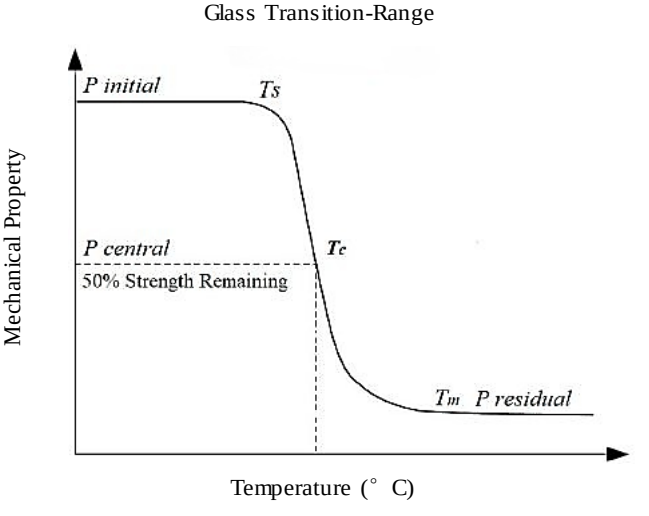


**Fig. 1** Relationship between FRP mechanical properties and temperature. Reproduced with the Permission from [35] Copyright 2014 WILEY-VCH Verlag GmbH & Co. KGaA, Weinheim.

The overall performance of FRP under elevated temperatures are categorized into two types: a) FRP elements directly exposed to heat flux and fire (*e.g.* Bridge piers).[36–40] b) FRP elements not in direct contact with heat flux and fire (*e.g.* concrete members reinforced with FRP bars).[41–45] In addition to the above types, based on different applications, some factors affecting FRP performance at variable temperature also include type and configuration of fibres, resin, and the manufacturing process used for fabricating FRP structures.

The different degradation mechanisms at different temperature ranges are: 1) The failure mode is brittle when the FRP structure is exposed at a temperature below that of glass transition temperature ($T_g$) as fibers are still intact and

surrounded by resin matrix. 2) as the temperature reaches glass transition, the resin changes its state as explained above and softens, causing gasification followed by fibre rupture.[46] 3) when the temperature exceeds the decomposition temperature ($T_d$), resin's self-ignition occurs, and due to no resin, only the fraction of fibres remain.[47]

The scanning electron microscopic (SEM) images of affected FRP laminates at different temperatures are shown in Fig. 2. As seen in Fig. 2(a) at room temperature, the fibres are bounded by matrix, and there are no modifications in the composite surface. As the temperature increases (*i.e.* at moderate temperature from Fig. 2(b)), the matrix softens and degrades with fibres becoming more visible. At extreme temperatures from Fig. 2(c), the matrix is completely burnt off, remaining with only fibres.

## 3. Mechanical properties

FRP composites are largely used to enhance the mechanical properties of concrete structures, columns, slabs. Therefore, a thorough understanding of FRP composites' high-temperature behavior and mechanical performance is essential. In thermoset composite materials, the factors affecting heat propagation are fiber orientation, configuration, and volume fraction.[49,50] Moreover, investigations performed under cryogenic temperature also showcase the propagation of microcracks at the fibre/matrix interface, resulting in debonding and delamination.[51–55] This section briefly discusses the tensile, flexural, interlaminar and compressive properties performed on various FRP composites.

### 3.1 Tensile properties

Many researchers have focused on experimental and numerical analysis, on a diverse range of FRP laminates, based on a different orientation, thickness, resin types at temperatures from ambient to fire condition. From the results obtained, researchers have developed and proposed several prediction models by establishing the relation between the mechanical properties of FRP composites at elevated temperatures. In the present section, various researchers determining tensile properties at temperatures (200 to 700 °C) are explained, whereas, the numerical models are presented in the next section.

Jafari *et al*.[25] investigated the tensile properties of uni-directional, woven, and chop strand mat glass fibre laminates at high temperatures. The effect of laminate thickness and fibre orientation on tensile property were determined. According to their study, superior results were obtained for uni-directional fibre maintaining the tensile strength of 40% at 550 °C. However, laminates with woven and chop strand mat fibres lost all their tensile strength at temperatures 550 and 400 °C. Similarly, Jarrah *et al*.[56] found that a maximum reduction in tensile strength of 87% was obtained for glass fibre reinforced polymer (GFRP) composites whereas, a 67% reduction was observed for CFRP composites when tested at 600 °C.

Cao *et al*.[57] examined the tensile property of CFRP and hybrid glass/ basalt sheets subjected to a temperature of 200 °C. They determined; tensile strength was reduced to 40% at that respective temperature. In the further study, CFRP sheets were subjected to a temperature range of 20 to 120 °C as shown in Table 1. Below the glass transition temperature, stable behavior was detected, and a swift drop in tensile strength was observed when subjected to the above glass transition temperature. In case of woven GFRP composites subjected to a temperature of 300 °C, 80% reduction in strength was reported by Gibson *et al*.[58]. According to the investigation of Kumarasamy *et al*.[59] on determining the tensile strength of GFRP laminates fabricated using hand lay-up, at a testing temperature of 25 to 80 °C. From the results obtained, maximum of 65% strength reduction was noted at 80 °C. During the investigation by Hawileh *et al*.[60] on carbon, basalt, and carbon/basalt hybrid laminates. 90% reduction of tensile strength was noted at laminates exposed to a temperature of 250 °C. In their further study, carbon, glass, and hybrid laminate of carbon/glass were investigated above the same temperature. They saw an improved performance (*i.e.*, the elastic modulus reduction of 9% for hybrid glass/carbon in comparison to 28 and 26% for glass and carbon laminates, respectively) at 250 °C. Extensive literature performed by Bazli and Abolfazli[48] on the investigation of tensile properties on FRP laminates reported that the maximum tensile strength retention was obtained between the temperature of 200 to 300 °C for CFRP and GFRP laminates as represented in Fig. 3. They also concluded that the result

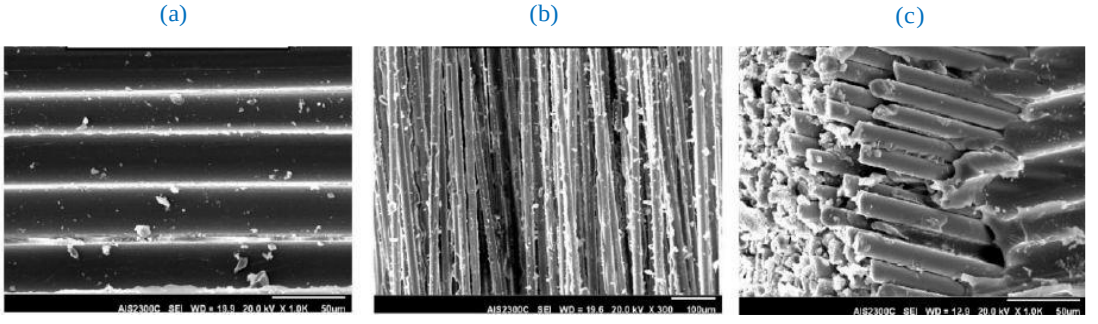


**Fig. 2** SEM images of composite exposed at: (a) room temperature, (b) moderate temperature and (c) high temperature.[48]

 

**Table 1.** Tensile properties at elevated temperatures.

| Ref. | Fibre Type | Resin Type | Fabrication Method | Glass Transition Temperature $T_g$ (°C) | Testing Temperature (°C) | Outcomes |
|---|---|---|---|---|---|---|
| Cao *et al*.[57] | UD E-Glass, UD Carbon | Epoxy | Hand lay-up | 38 | 40, 80, 120, 160, 200 | 1. Constant value of tensile strength (3000 MPa) at temperature (55 to 200 °C) for CFRP.<br>2. Hybridization of carbon/glass fibre improved tensile properties at elevated temperature.<br>3. 68% tensile strength retention at 16 °C for hybrid composites at elevated temperatures. |
| Hawileh *et al*[60] | UD Carbon | Epoxy | Hand lay-up | 85 | 25, 100, 200, 250 | 1. Tensile strength (578 MPa) and elastic modulus (37.258 GPa) were maximum at room temperature (25 °C) .<br>2. Minimum tensile strength (112 MPa) and elastic modulus (3.382 GPa) at (250 °C). |
| Hawileh *et al*.[70] | UD carbon, UD glass | Epoxy | Hand lay-up | NA | 25, 100, 150, 200, 250, 300 | 1. At (25 °C) Maximum tensile strength (1485 MPa) and (46.277 GPa) tensile modulus.<br>2. At temperature (300 °C) minimum of (802 MPa) tensile strength and (17.935 GPa) of elastic modulus for UD carbon.<br>3. For UD glass<br>At (25 °C) Maximum (1365 MPa) tensile strength and (38.999 GPa) tensile modulus and at temperature (300 °C) minimum tensile strength of (772 MPa) and (27.300 GPa) of elastic modulus.<br>4. Tensile strength and modulus reduced to 42% and 9% for UD carbon at 250 °C.<br>5. For UD glass, strength and modulus reduction was 31% and 26% at 250 °C. |
| Jafar *et al*.[25] | UD glass, Woven glass, Chopped strand mat glass | Epoxy | Vaccuum infusion process | 70 | 25, 60, 80, 105, 150, 200, 250, 300, 400, 550 | 1. From 25 to 75 °C ($T_g$), very slight decrease in strength and modulus.<br>2. Above 75 to 150 °C significant decrease in strength and modulus.<br>3. Above 150 °C rapid degradation of resin and load carrying capacity is entirely on fibres.<br>4. Higher tensile strength and |

**Continued**

| | | | | | | |
|---|---|---|---|---|---|---|
| | | | | | | modulus was seen for UD laminates, followed by woven laminates and least by randomly distributed laminates. |
| Ashrafi *et al.*[71] | UD glass, Woven glass, Chopped strand mat glass | Epoxy | Vaccuum infusion process | 70 | 25, 70, 120, 200, 300 | 1. For unconditioned samples (without thermal treatment) at lower thickness woven laminates and random laminates exhibited lower tensile strength.<br>2. For conditioned samples, tensile strength reduced with increasing exposure time (120 min).<br>3. Less significant effect of elastic modulus and tensile strength below 120 °C. |
| Jarrah *et al.*[56] | Woven carbon, Woven glass | Epoxy | Hand lay-up | 60 | 25, 60, 100, 150, 200, 250, 300, 350, 400, 450, 500, 600 | 1. About 87% for woven CFRP and 67% for woven GFRP laminates, reduction in tensile strength at 600 °C. |
| Wang *et al.*[47] | UD carbon | Epoxy | Pultrusion process | 60 | 22, 50, 103, 155, 211, 308, 420, 520, 625, 706 | 1. Slight reduction in tensile strength at temperature 20 to 150 °C.<br>2. Only 7% strength retention at 700 °C compared to room temperature.<br>3. Self-ignition of laminates at temperature range 350 to 600 °C. |
| Lu *et al.*[46] | UD glass | Epoxy | Pultrusion process | 167 | 25, 40, 80, 120, 160, 200 | 1. With the increase in exposure time, tensile strength reduction ranged from 3.9% to 43.2%. |
| Gibson *et al.*[58] | UD glass | Polypropylene | Vaccuum bagging process | NA | 20, 40, 60, 80, 100, 120, 140, 170 | 1. Tensile strength dropped significantly from 20 °C.<br>2. For 12 mm thick laminates, tensile stress results under heat flux (50 kW/m$^2$) is quantitatively nearer to thermosetting laminates. |
| Cao *et al.*[72] | UD carbon | Epoxy | Hand lay-up | 45 | 20, 30, 35, 40, 45, 50, 55, 60, 70, 80, 100, 120, 140 | 1. Average tensile strength and elastic modulus of 4127 MPa and 254.2 GPa obtained at room temperature (20 °C).<br>2. Rapid reduction in tensile strength at temperature 40 to 60 °C.<br>3. Above 60 °C, average tensile strength loss is nearly stable. |
| Shekarchi *et al.*[67] | UD carbon, UD glass | Epoxy | Hand lay-up | 100 | 25, 100, 150, 200, 250, 300, 350, 400, 500 | 1. Ultimate tensile strength initially maximum at room temperature (25 °C) for GFRP.<br>2. With increasing temperature |

**Continued**

| | | | | | | |
|---|---|---|---|---|---|---|
| | | | | | | CFRP is more stable compared to GFRP in terms of tensile strength. |
| Aydin[73] | UD glass | Polyester | Pultrusion process | NA | -50, -25, -10, 0, 10, 25, 50, 75, 100, 125, 175, 200 | 1. Maximum tensile strength at 25 °C (351 MPa), least strength at 200 °C (186 MPa).<br>2. From 0 to -50 °C, tensile strength decreased in a constant level.<br>3. Stress strain curves represent increase in brittleness at temperature below 0 °C and reduced rigidity at temperatures above 50 °C. |
| Chowdhury *et al*.[74] | UD glass | Epoxy | Hand lay-up | 75 | 20, 45, 60, 75, 90, 200 | 1. Tensile strength loss at 60 °C is 51% and elastic modulus loss is 70%. |
| Yu and Kodur[75] | UD carbon | Epoxy | Pultrusion process | 80 | 20, 100, 200, 300, 400, 500, 600 | 1. Tensile strength retention of about 80% at temperature range of 20 to 200 °C.<br>2. Rapid degradation of tensile strength at temperature range of 200 to 400 °C.<br>3. In temperature 500 to 600 °C, only 10% strength retention is noted. |
| Foster and Bisby[61] | UD carbon, UD glass | Epoxy | Hand lay-up | 78 | 20, 100, 200, 300, 400 | 1. CFRP samples retained its tensile strength upto 300 °C.<br>2. Significant loss in tensile strength noted for GFRP samples from 200 °C. |
| Kumarasamy *et al*.[59] | Woven glass | Polyester | Hand lay-up | NA | -20, -15, -10, -5, 25, 40, 50, 60, 80 | 1. With increase in temperature (40 to 80 °C), strength and modulus decreased due to resin softening.<br>2. Slight increase of tensile modulus from 25 to -5 °C, from -5 to -20 °C slight decrease in modulus. |
| Park *et al*.[65] | Neat CFRP chips, Recycled carbon fibre chips | Phenolic | Resin infusion | 300 | 25, 300, 400, 500, 600 | 1. Thermally treated (400 °C) recycled-CFRP phenolic chip composites exhibited higher tensile properties. |
| Reis *et al*.[66] | Glass fibre | Epoxy | Hand lay-up | 60 | 20, 40, 60, 80 | 1. Modulus of elasticity decreased to 5.4%, 35.6% and 54.4% at 40, 60 and 80 °C. |
| Nguyen *et al*.[68,69] | Carbon fibre | Epoxy | Hand lay-up | 82 | 20, 200, 400, 600 | 1. The maximum tensile strength at 350 °C, decreased by 50%.<br>2. Tensile modulus at 600 °C, decreased by 30%. |

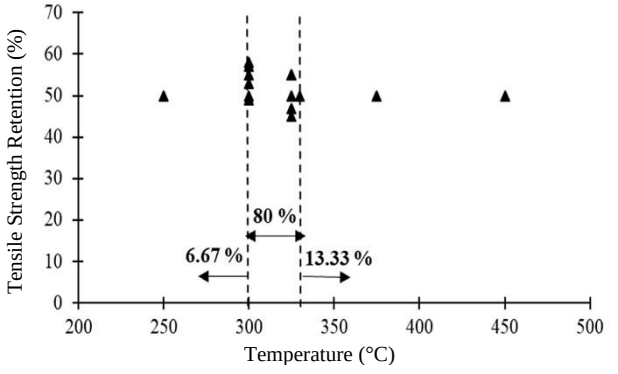


**Fig. 3** Tensile strength Vs. the critical temperature performed in the literature by Bazli and Abolfazli. Reproduced with the Permission from [48], Copyright 2020, Multidisciplinary Digital Publishing Institute.

values obtained were more scattered, as the fabrication technique selected differed from one researcher to another.

Uni-directional (UD) CFRP laminates aged for period of 555 h at a cryogenic temperature of -184 °C presented a 20% decrease in tensile strength compared to specimens exposed to room temperature.[52] In the study of Foster and Bisby[61] no loss in tensile strength was observed for CFRP composites until 300 °C, however above 300 °C there was rapid reduction as shown in Fig. 4(a). However, in case of GFRP composites reduction was observed at the beginning of 200 °C as seen in Fig. 4(b). Failure tensile specimens of CFRP and GFRP exposed at 20, 100, 200, 300 and 400 °C are shown in Fig. 5.

Tensile behavior of CFRP sheets in the temperature range of 20 to 60 °C for different types of resins were investigated by Wu *et al*.[62]. Tensile modulus was increased for thermally treated CF T300 at 1500 °C, with the minimum modification in surface morphology. Thermally-treated carbon fibres' displayed good thermal and mechanical stability by improving their graphitization degree at elevated higher temperatures.[63] Likewise, thermal decomposition of glass/vinyl ester (VE), glass/polyester (PE), and glass/polypropylene (PP) for tensile strength estimation at temperature 0 to 200 °C displayed a similar failure behavior for the same strain rate. However, compressive strength was lower than tensile strength and was below zero for glass/PP as soon as the temperature exceeded the melting point of PP.[64]

Mechanical and thermal analysis was performed by thermally treating recycled carbon fibre (RCF) chips for 2 h at temperature ranging from 100 to 600 °C into the phenolic resin by Park *et al*.[65] Mechanical properties explored at temperature condition of 60 °C presented best result of tensile strength for thermal treatment at 400 °C of recycled carbon fiber chips as represented in Fig. 6. In Fig. 6, different abbreviations are as follows PR-Phenolic resin, NCPC- Neat CFRP chip-phenolic composite, CPC- CFRP chip phenolic composites at different thermal treatment conditions (*i.e.* 200, 300, 400, 500 and 600 °C).

Reis *et al*.[66] studied the tensile performance of GFRP laminates at a ambient temperature to 80 °C, at different strain rates. They concluded that the strain rate played a significant factor in influencing the tensile performance of GFRP. However, no influence was seen on elastic modulus due to variable strain rate. The investigation of ultimate tensile strength for CFRP and GFRP laminates at temperature 25 to 500 °C by Shekarchi *et al*.[67] found a strength reduction of 83% for GFRP and 70% for CFRP laminates at 500 °C. They also reported that for exposed temperature of 200 °C, 48 and 39% reduction was noted.

Based on the fire application Nguyen *et al*.[68,69] conducted an experimental investigation on manually fabricated hand lay-up CFRP (M-CFRP). Two types of thermo-mechanical tests were performed: constant temperature test to determine Young's modulus, ultimate strength, and later a constant mechanical load test to determine the failure temperature of M-CFRP. The temperature levels selected for the experiment were 20 to 600 °C. With increasing temperature, 50% loss in ultimate strength was reduced, followed by a 30% reduction in Young's modulus. The rapid drop was observed between 20 to 200 °C. However, there was a gradual decrease in strength and Young's modulus for the temperature range of 400 to 600 °C. Also, a correlation was established between temperature and mechanical loading of M-CFRP in the same study.

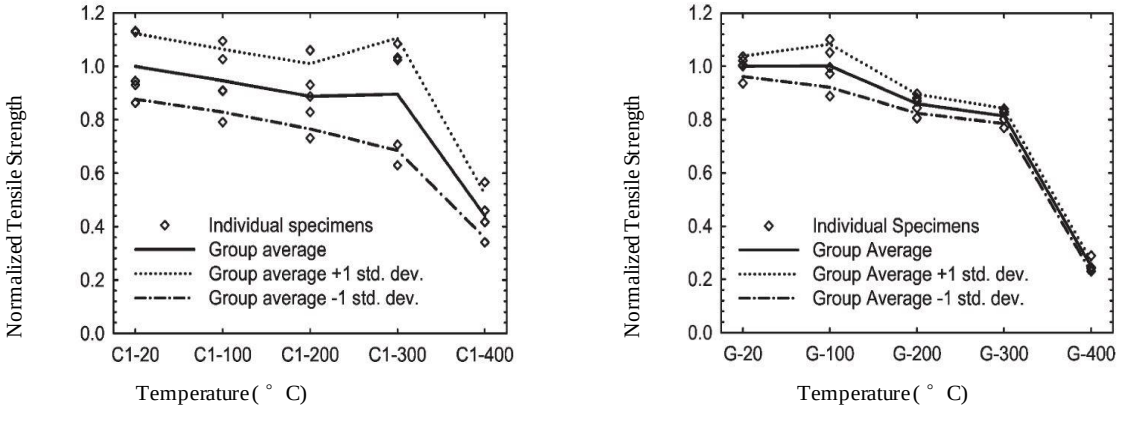


**Fig. 4** Variation in ultimate tensile strength of (a) CFRP specimens and (b) GFRP specimens exposed at elevated temperatures. Reproduced with the permission from [61], Copyright 2005, Farmington Hills, Mich. American Concrete Institute.

 

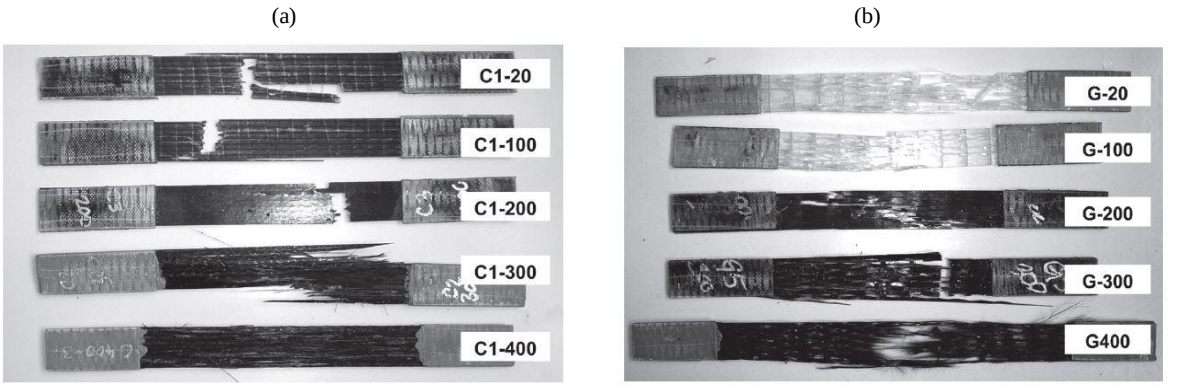


**Fig. 5** Failure tensile specimens of (a) CFRP and (b) GFRP at elevated temperatures. Reproduced with the permission from [61], Copyright 2005, Farmington Hills, Mich. American Concrete Institute.

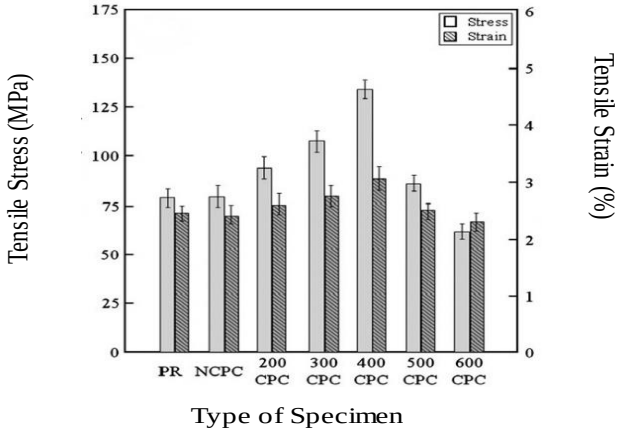


**Fig. 6** Tensile property of thermally treated recycled carbon fiber chip–phenolic composite at 60 °C. Reproduced with the permission form [61]. Copyright 2012 SAGE Publications.

### 3.1.1 Tensile properties-predicting numerical models at various temperatures

During designing of composite structures, systematic study on the behavior of structures at elevated temperatures is necessary. Researchers have proposed numerical models for predicting tensile properties of FRP's. Gibson *et al*.[76] were the first to propose a primary model for predicting mechanical properties at elevated temperatures. By further implementing Gibson *et al*. model, several researchers proposed various numerical models for detecting mechanical properties of FRP's as explained below.

$$P(T) = \frac{P_u+P_R}{2} - \frac{P_u-P_R}{2} erf\left(k(T-T')\right) \quad (1)$$

$$P(T) = \frac{P_u+P_R}{2} - \frac{P_u-P_R}{2} tan\ h\left(k(T-T')\right) \quad (2)$$

Eqs. 1 and 2 represent the Gibson *et al*. numerical model. The specific property (tensile or compressive) to be determined is denoted by P (T). $P_u$ and $P_R$ represent unrelaxed property at low temperature and relaxed property at high temperature, k represents distribution constant, erf and tan h represents the error and hyperbolic tangent function and T' being determined respective glass transition temperature of composite.

By implementing regression analysis to achieve a minimum error of the Gibson *et al*. model, Yu and Kodur[75] developed new equations for determining the tensile strength R(T) and elastic modulus R(E) of CFRP pultruded strips, as represented in Eqs. 3 and 4. Eqs. 5 and 6 also represent tensile strength and modulus for CFRP pultruded rods. Tan h represents the hyperbolic tangent function.

$$R(T) = 0.56 - 0.44\ tan\ h(0.0052(T-305)) \quad (3)$$

$$R(E) = 0.51 - 0.49\ tan\ h\ (0.0035(T-340)) \quad (4)$$

$$R(T) = 0.54 - 0.46\ tan\ h(0.0064(T-330)) \quad (5)$$

$$R(E) = 0.51 - 0.49\ tan\ h\ (0.0033(T-320)) \quad (6)$$

They discovered an average error of 7% and 6.3% between the predicted tensile strength obtained from the developed model and experimental tests performed on pultruded CFRP strips and rods.

A similar study was performed by Saafi *et al*.[45] to determine the tensile properties of GFRP bars at various temperature conditions. Eqs. 7 and 8 represent the numerical model used for predicting the tensile strength R(T) and elastic modulus R(E).

$$R(T) = 1 - 0\ .0025\mathrm{T} \qquad \{0 \le \mathrm{T} \le 400\ °\mathrm{C} \quad (7)$$

$$R(E) = \begin{cases} 1 & 0 \le T \le 100\ °C \\ 1.25 - 0.0025T & 0 \le T \le 300\ °C \\ 2 - 0.005T & 300 \le T \le 400\ °C \end{cases} \quad (8)$$

For determining the tensile strength R(T) of CFRP laminates, Wang *et al*.[47] developed a stress-temperature relation model, as represented in Eq. 9.

$$R(T) = \begin{cases} 1 - \frac{(T-22)^{0.9}}{200} & 22 \le T \le 150\ °C \\ 0.59 - \frac{(T-150)^{0.7}}{490} & 150 \le T \le 420\ °C \\ 0.48 - \frac{(T-420)^{1.8}}{76000} & 420 \le T \le 706\ °C \end{cases} \quad (9)$$

### 3.2 Flexural properties

Numerous researchers investigated the temperature effect on flexural and interlaminar shear strength of FRP laminates. Ningyun and Evans[77] performed the first study on graphite fibre laminates to determine the flexural properties by conducting a short beam shear test at temperatures up to 300 °C. They found that the decrease in temperature leads to delamination fracture. A maximum strength loss of about 75% was observed at temperature 300 °C. During the investigation of laminate thickness and fibre orientation effect on flexural

strength of GFRP laminates at various temperatures. The authors reported that thinner laminates were more vulnerable at temperature 300 °C than thicker laminates. Also, in fibre orientation, maximum strength was retained for uni-directional fibres compared to laminates fabricated with woven and chopped strand mat fibres. In the study of Shekarchi *et al*.[67] flexural strength reduction of 89% was obtained for CFRP exposed to temperature at 350 °C. For the same condition, maximum of 93% strength reduction was noted for GFRP laminates. A similar experimental study was performed on pultruded GFRP laminates by Vieira *et al*.[78] at laminates exposed to a maximum temperature of 320 °C. The authors declared no considerable reduction in flexural (*i.e.* 25%) and interlaminar shear strength (*i.e.* 12%). In the further study of Schmidt *et al*.[79] pultruded GFRP laminates with isophthalic polyester and phenolic resins exposed to elevated temperatures found that GFRP laminates with phenolic resins showed better results as compared to the latter type.

Similar outcomes were reported for CF/epoxy by Aoki *et al*.[80] when influenced at -269 °C, claiming crack initiation taking place at lower load level than at room temperature. Using liquid nitrogen, interlaminar shear stress (ILSS) for woven and chopped E-glass fibre/epoxy, and woven CF/epoxy was investigated by Surendra *et al*.[81,82] An increase in ILSS was observed as the load transfer arrest seen through the glass fibre/matrix interface due to the hardening of the matrix at a lower temperature.[83] However, in CF/epoxy, due to its anisotropic nature, contraction of carbon fibre was experienced in the transverse direction at the cryogenic condition resulting in a weak interfacial bond leading to a decrease in ILSS.[51]

The bending strength of CF/epoxy was studied under the thermal treatment for the temperature ranges as mentioned in Table 2. Bending strength was found to be maximum for 120 to 150 °C and was relatively stable in the temperature range of 20 to 90 °C, with the least strength observed at 120 °C. At 120 to 150 °C, the secondary curing enhanced the resin's cross-linking density, resulting in increased bending strength of 3.11% higher. Extreme bending failure was observed at 150 °C as shown in Fig. 7, and with increasing temperature, the loss was tangible.[84]

**Table 2.** Flexural properties at elevated temperatures.

| Ref. | Fibre Type | Resin Type | Fabrication Method | Glass Transition Temperature $T_g$ (°C) | Testing Temperature (°C) | Outcomes |
|---|---|---|---|---|---|---|
| Shekarchi *et al*.[67] | UD carbon, UD glass | Epoxy | Hand lay-up | 100 | 25, 100, 150, 200, 250, 300, 350 | 1. Flexural strength retention at 250 °C for UD carbon is 50%.<br>2. Flexural strength retention of 50% for UD glass noted at 250 °C.<br>3. At maximum temperature strength retention is 11% and 7% for UD carbon and glass. |
| Bazli *et al*.[86] | UD glass, Woven glass, Chopped strand mat glass | Epoxy | Vaccuum infusion process | 70 | 25, 70, 120, 200, 300 | 1. Uni-directional composites exhibited superior strength corresponding to woven and randomly oriented composites at elevated temperatures.<br>2. 5% decrease in flexural strength at temperature 60 to 200 °C, 90% reduction in temperature 200 to 300 °C. |
| Manalo *et al*.[87] | UD glass, Woven glass, Chopped strand mat glass | Phenolic | NA | 93 | 21, 35, 50, 65, 80, 100, 120, 150, 180 | 1. Flexural strength retention of about 60% upto 80 °C.<br>2. 80% retention of modulus from room (21 °C) to maximum temperature |

**Continued**

| | | | | | | |
|---|---|---|---|---|---|---|
| | | | | | | (180 °C). |
| Vieira *et al*.[78] | Glass fibre | Isothalpic polyester, Vinylester, Phenolic | Pultrusion | 230 | 24, 120, 170, 220, 270, 320 | 1. At elevated temperatures vinylester composites presents the higher flexural strength.<br>2. Composites with isothalpic polyester showed the lowest modulus of elasticity. |
| Schmidt *et al*.[79] | E- Glass fibre | Isothalpic resin, Phenolic | Pultrusion | NA | 250 | 1. Isothalpic resin matrix composites presents decrease in flexural strength at shorter exposure duration 30 min.<br>2. Phenolic matrix composites show more thermal stability at 250 °C. |
| Aoki *et al*.[80] | Carbon fibre | Bismaleimide, Polyether ether ketone | NA | NA | -269, -169, 20 | 1. Fracture toughness is maximum at cryogenic condition (-269 and -169 °C), due to increase in matrix strength. |
| Surendra *et al*.[81,82] | Chopped E-glass | Epoxy | Hand lay-up | NA | -196 | 1. Composites in cryogenic condition shows immense matrix cracking and interfacial debonding as brittleness of matrix increases. |
| Wang *et al*.[88] | UD carbon | Epoxy | NA | 90 | 20, 60, 90, 120, 150, 180 | 1. Storage modulus and interfacial shear strength are in a steady state at temperature 20 to 95 °C.<br>2. At temperature 95 to 120 °C, modulus and interfacial shear strength declines at a rapid rate. |

UD- Uni-directional.

Interlaminar strength was studied by Li *et al*.[85] performing a microwave curing process, to achieve stronger interface bonding between fibers and fillers. An overall, 66% increase in mode-1 interlaminar fracture toughness for microwave curing was observed compared to the traditional curing process. A 16% decrease in delamination factor was perceived in hybrid composite in comparison to the neat CF/epoxy composites.

Wang *et al*.[88] investigated UD carbon fiber epoxy under temperature-controlled conditions. The temperature range selected for the study was 23 to 120 °C, with a 30 °C increment. At 23 to 95 °C, steady behavior was observed in storage modulus and interfacial shear strength (IFSS). However, above 95 °C, a sharp decline was observed as the matrix was in the glass transition temperature range.

### 3.3 Compressive Properties

Compared to investigating tensile and flexural properties at elevated temperatures, the experimental study performed on compressive properties is limited. The limitation for lower analysis is that more research is required to understand laminates' local and global buckling behavior when undergoing compressive tests at different temperatures.

During the investigation of compressive property for woven glass fibre composites with polypropylene matrix subjected to fire condition. Gibson *et al*.[58] concluded that at the temperature exposure of 140 °C, compressive strength reduced to 90%. Similarly, On the application of combined

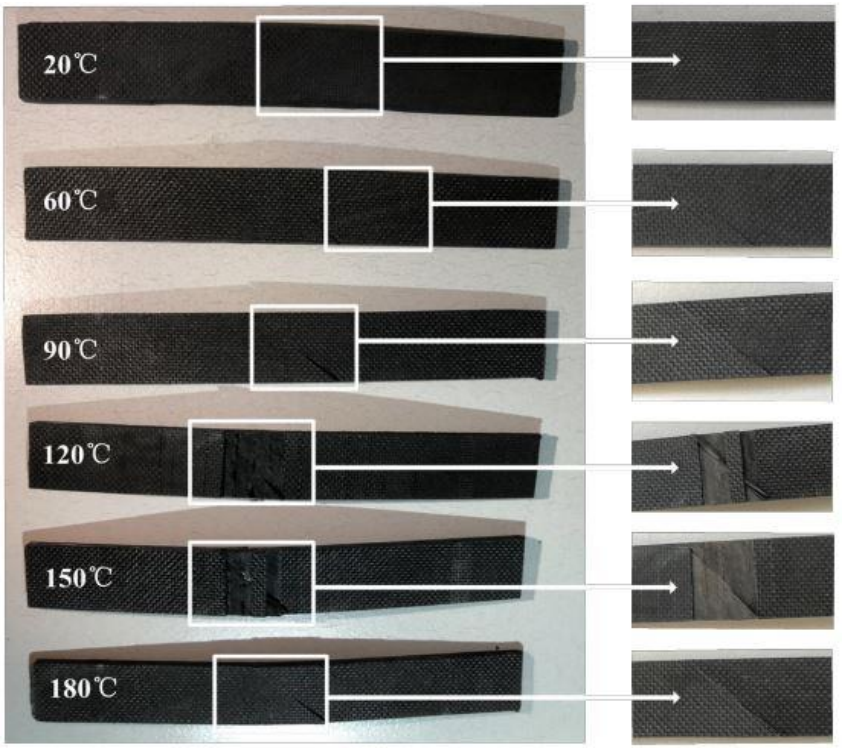


**Fig. 7** Bending deformation of CFRP at different temperatures. Reproduced with the Permission from [84]. Copyright 2019, De Gruyter.

thermal and compressive load on FRP composites, Asaro *et al*.[89] determined two important factors, stating that degradation of composites, the strength, and failure significantly depends on the exposure time and the temperature subjected on the composites. Table 3 represents compressive properties at different testing temperatures.

## 4. Machining of composites

Although fabrication is performed to the near net shape of FRP composites, the machining operations are still necessary to finalize the part sizes and accomplish a close tolerance fit.[91] The machining of FRP composites differ from those of traditional metals.[92] In machining of FRP composites for aerospace parts, the demand for excellent surface quality and geometric dimensional stability is of utmost necessity for the proper functioning of components and safety necessities.[93]

**Table 3.** Compressive properties at elevated temperatures.

| Ref. | Fibre Type | Resin Type | Fabrication Method | Glass Transition Temperature $T_g$ (°C) | Testing Temperature (°C) | Outcomes |
|---|---|---|---|---|---|---|
| Gibson *et al.* [58] | Woven glass | Polypropylene | Vaccuum bagging process | NA | 20, 40, 60, 80, 100, 120, 140, 170 | 1. Compressive strength at 0 °C is 260 MPa and at 130 °C strength decreases to 68 MPa.<br>2. Strength value at 160 °C is zero at the melting point of polypropylene matrix. |
| Feih *et al.* [90] | Woven glass | Vinylester | Vaccuum bagging process | 120 | 50, 100, 150, 200, 250 | 1. Compressive strength at room temperature is 435 MPa.<br>2. Above 50 °C, compressive strength degrades rapidly. |
| Park *et al.* [65] | Neat CFRP chips, Recycled carbon fibre chips | Phenolic | Resin infusion | 300 | 25, 200, 300, 400, 500, 600 | 1. Maximum compressive strength (210 MPa) obtained for thermally treated (400 °C) neat CFRP chip composites. |

CFRP- Carbon fibre reinforced polymer.

 

Many attempts have been performed to achieve the above goal by introducing various new technologies, for instance, vibration-assisted machining,[94–96] ultrasonic-assisted machining,[97–99] modulation assisted machining (MAM),[95,100,101] laser-assisted machining,[102,103] vibration-assisted drilling (VAD)[104–106] and orbital drilling processes.[107,108] However, the challenges of machining have always remained disputed, as the behavior of composites is inconsistent due to their inhomogeneity, abrasiveness, and anisotropic nature. Several types of tool materials are used to maintain the output quality of machined composite parts. According to Saoubi *et al*.[109] tool materials for machining of composite components are classified into two categories:

a) Carbides (cemented and coated) and ceramic tools fall under hard materials due to their high fracture toughness and good thermal stability.
b) Polycrystalline diamond (PCD) and cubic boron nitride (CBN) are considered super-hard to display extreme hardness and thermal conductivity during machining.

### 4.1 Temperature influence on machining of composites

Based on various applications of composite materials exposed to a diversity of environmental conditions, recently, researchers have made numerous attempts to study the environmental factors (moisture, ultraviolet radiation, and extreme fluctuating temperatures) affecting FRP composites' performance.[5,110–115] Several studies are performed on characterizing the outcome of fire and thermal loads affecting mechanical properties of composite materials as explained in the above sections. However, the difficulty in experimentation and the indeterminate flammable nature of polymer composites are still dubious.[90,116–120] During the machining of composite materials, high cutting temperatures cause heat-affected zones (HAZ), which extremely impacts the performance of fabricated composite parts.[121]

The critical temperature of 180 °C is produced during the cutting process of CFRP/epoxy composites.[122] The research on this topic is limited, as the challenge always exists in eliminating the thermal effect induced machining composites. This section summarizes the thermal effect and the outcome of temperature generated during the machining of FRP composites.

#### 4.1.1 Orthogonal cutting

In orthogonal cutting of composites, as the cutting temperature exceeds the glass transition temperature of the matrix, the irreversible mechanical, chemical, and thermal decomposition affects the functioning of components.[123–125] This, in turn, increases cost of the components as the rejection of parts becomes higher.[126,127] Characterization of homogeneous materials during cutting is done due to plastic deformation producing continuous chips. Different conventional machining performed by the researchers to study the thermal effect on composites is tabulated in Table 4.

Orthogonal cutting was first applied to FRP's by Koplev *et al*.[128] to study the formation of chips and wear of the tool. The influence of workpiece temperature was discussed by Brinksmeier *et al*.[108] and Pecat *et al*.[129] on machining quality. The results from their investigations exposed the relation of depth of HAZ with the length of bending carbon fiber, representing the cutting induced damage. UD CF's cured at different temperature conditions showed no influence on surface roughness ($R_a$) during orthogonal machining.[130] Wang *et al*.[121] claimed the effect of fibre orientation on cutting temperature during dry orthogonal cutting of CFRP. A new approach of heat partition ratio was implemented for machining composites, obtained from the analytical model, latter was added to a finite element model. Then, the numerical results were validated to experimental outcomes. The maximum cutting temperature was observed for 90° fibre orientation, as shown in Fig. 8. Thermal effects were predicted by developing a three-dimensional (3D) finite element model of orthogonal cutting of CFRP composite laminates. For the fibre orientation of -45 and 90°, higher thermal damage was noted as the cutting speed increased from 300 to 600 m/min, whereas damage was seen with the increasing cutting speed from 60 to 6000 m/min.[131]

**Table 4.** Temperature influence on different conventional machining performed in the literature.

| Fibre Type | Machining Method | Ref. |
|---|---|---|
| CFRP | Orthogonal Cutting | Wang *et al*.[121], Wang & Zhang[130], Santiuste *et al*.[131], Yan *et al*.[147], An *et al*.[148] |
| | Milling | Morkavuk *et al*.[142], Cui *et al*.[141], Ghafarizadeh *et al*.[149], Yashiro *et al*.[150], Liu *et al*.[151], Kerrigan *et al*.[152], Khairusshima *et al*.[153], Jia *et al*.[154], Gao *et al*.[155] |
| | Drilling | Wang *et al*.[88], Brinksmeir *et al*.[108], Joshi *et al*.[156], Kumaran *et al*.[157], Merino-Perez *et al*.[158], Alvarez *et al*.[159], Sorrentino *et al*.[160], Saleem *et al*. [161], Nagaraj *et al*.[162], Ferreira *et al*.[163], Ben *et al*.[164] |
| GFRP | Drilling | Loja *et al*.[165], Sorrentino *et al*.[160] |
| | Edge Trimming | Jamal Sheikh *et al*.[166] |

CFRP- Carbon fiber reinforced polymer; GFRP- Glass fiber reinforced polymer.

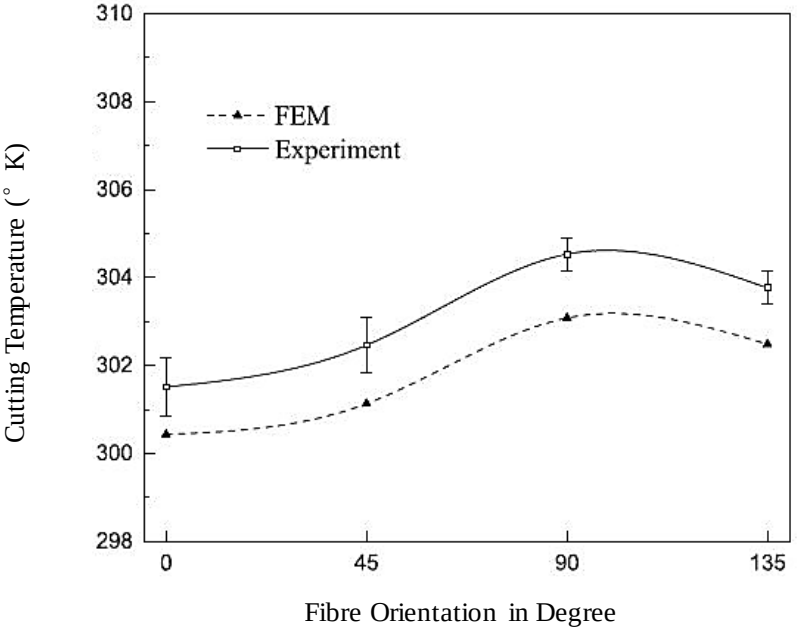


**Fig. 8** Maximum cutting temperature measured at different fibre orientations of UD-CFRP. Reproduced with the Permission from [121]. Copyright 2018 Elsevier Ltd.

### 4.1.2 Milling and edge-trimming

Milling is one of the advanced machining methods applied for hole making, slots, and keyways in hard materials, such as titanium (Ti) alloy, aluminum alloy, and CFRP composites.[132–137] Researchers are trying to reduce the thermal defects and surface-induced damage by employing mathematical models to predict the temperature distribution in milling of CFRP composites.[138–141] Other approaches such as cryogenic cooling, minimum quantity lubrication (MQL), flood cooling have also been studied for reducing heat generation during milling of composites.[142–146]

Ghafarizadeh *et al*.[149] reported a maximum cutting temperature observed for 90° fibre orientation during milling of CFRP. Also affirming, fibre orientation and cutting speed being significant factors on affecting cutting temperature. In the work of Yashiro *et al*.[150] cutting temperatures during end milling was studied by employing three different types of measuring methods. The first method was analysed using an infrared camera, secondly using a tool-workpiece thermocouple, and later by thermocouples embedded between different composite layers. The authors reported, at a cutting speed of 25 m/min, the cutting temperature at the tool-workpiece interface measured 180 °C, and with the increasing cutting speed of 100 m/min, cutting temperature reached 300 °C. The cutting temperature remained stable with the furthermore increase in the cutting speed. Moreover, comparing temperature at the contact point to that of the workpiece material, a minimum cutting temperature was achieved at a high cutting speed of 300 m/min.

Similarly, Liu *et al*.[151] studied the variation of workpiece temperature during helical milling of CFRP composites. The authors concluded that the effect of axial cutting depth had a maximum influence on the variation of workpiece temperature compared to the spindle speed. Kerrigan *et al*.[152] specified the workpiece thickness and depth of cut being the vital parameters that significantly influence cutting temperature. A comparison study on surface roughness produced by performing milling of CFRP laminate at room temperature by supplying chilled air of -10 °C was investigated by Khairusshima *et al*.[153] Minimum surface roughness was reported for chilled air condition at the lowest feed of 0.025 mm/rev with a constant cutting speed of 179 m/min. Influence of cutting area temperature maintained at two temperature range -50 to -25 °C and -10 to 25 °C using cryogenic nitrogen gas, on surface integrity was investigated by Zhenyuan Jia *et al*.[154] during an end milling operation of multidirectional CFRP. The results represented, that the material removal was uniform under low temperatures and uneven removal and maximum surface roughness were observed with increasing temperatures. Furthermore, the authors added that the effect of the flow rate and pressure of nitrogen gas has a significant influence in reducing the surface roughness during the process.

Heat partition and temperature distribution were investigated by Jamal Sheikh *et al*.[166] by edge trimming operation of GFRP laminate, adopting the inverse heat conduction method. The authors concluded that no machining thermal damage was produced due to low temperature and shorter exposure time. However, the maximum surface area temperature was determined to be 178 °C, falling below the glass transition temperature of epoxy.

### 4.1.3 Drilling

For decades, drilling has been the most commonly used conventional methods for producing holes in composites. Damage suppression strategies during the drilling of composites have been a continuous research topic drawing the

 

attention of all the research community. Delamination, fibre pull out, and thermal ablation caused during drilling has been the high-risk factors for the continuous performance of components during its service life cycle.[167–172] From literature, to compute the damage, some studies propose different mathematical models,[173–175] whereas others considered optimizing various drilling parameters.[176–179] Similarly, researchers have tried reducing the delamination in composites by adapting different types of drilling tools- twist drill, step drill, candlestick drill, dagger drill, multi-facet drill, and trepanning drill.[180,181] Also, reduction was achieved by optimizing drilling conditions such as variable cutting speed,[182,183] feed rate,[184–186] point angle,[187] drill diameter,[188] pre-drilled pilot holes[189] and support plates.[190]

Unlike the study on high-temperature drilling performance on CFRP composite, from the literature, there is inadequate information regarding the cryogenic drilling performance of GFRP composites. When a desired quality of hole is to be produced, efficient drilling is performed, reducing excessive tool wear.[184,191] Engineering materials under low temperatures produce more resistance to deformation than at higher temperatures. Researchers have compared their study by performing dry drilling,[192–195] wet drilling,[196,197] and cryogenic drilling,[156,197,198] on composites. From most of the above three drilling operations, cryogenic drilling exhibited better results, followed by dry and wet drilling. During the process, the coolant supplied near the tool and workpiece interface, reduces the temperature caused due to friction and indeed reduced the rapid tool wear.[156,198] Dry drilling and cryogenic drilling were performed on CFRP composites. Concluding, tool wear progression reduced to 25% in the case of cryogenic drilling.[199] A similar study was conducted by Kumaran *et al*.[157] on woven CFRP, adopting the cryogenic method with the aid of nitrogen coolant. Peel-up delamination was found to be reduced due to an increase in the transverse strength of the composite.

Dry and cryogenic drilling, a comparative study performed by Joshi *et al*.[156] using nitrogen as a coolant, reported thrust force increase, however, delamination was found to be decreased compared to dry drilling. The relationship of cutting speed with heat dissipation during drilling of CFRP was noted by Merino-Perez *et al*.[158] An analytical and experimental study was performed by Sadek *et al*.[200] to predict thermal damage and delamination in FRP's using twist and multi-facet drills. The experimental and analytical results were found to be in good agreement when validated. The authors claimed, both thermal damage and delamination can be anticipated using their analytical approach.

Wang *et al*.[88] proposed a new method to control the drilling temperature for improving the quality of drilled holes in CFRP. Four temperature conditions were chosen for the study (*i.e*. -50, -25, 0 and 23 °C). The drilling temperature measured during the experiment was 45, 73, 100, and 128 °C for the above temperature conditions. Drilling parameters selected for the study are represented in Table 5. Drilling temperature had a significant influence on the surface roughness ($R_a$). The minimum surface roughness value was obtained for drilling temperature of 73 °C. Surface roughness measured along the parallel and perpendicular hole axis direction provided a minimum value of 51.9% and maximum

**Table 5.** Different cutting conditions and temperatures (*i.e.* supplied and measured) for drilling.

| Ref. | Cutting Speed (m/min) | Feed Rate (mm/rev) | Temperature (°C) |
|---|---|---|---|
| Wang *et al.*[88] | 25 m/min | 0.02 mm/rev | Initial temp. = -50, -25, 0, 23 °C<br>Drilling temp. measured = 128, 100, 73, 45 °C |
| Brinksmeir *et al.*[108] | 40, 80, 120 m/min | 0.25, 0.2, 0.18 mm/rev | Drilling temp. measured<br>Maximum = 191.6 °C for 120 m/min cutting speed and 200 mm/min feed rate<br>Minimum = 112.9 °C for 40 m/min cutting speed and 500 mm/min feed rate |
| Joshi *et al.*[156] | 100,125,150 m/min | 0.03, 0.06, 0.09 mm/rev | Temp. supplied = -190 °C |
| Kumaran *et al.*[157] | 15, 28, 57 m/min | 0.01, 0.05, 0.1 mm/rev | Temp. supplied = -196 °C |
| Merino-Perez *et al.*[158] | 50, 100, 150, 200 m/min | 0.005 mm/rev | Tool temp. measured,<br>Maximum = 260 °C for 100 m/min cutting speed |
| Loja *et al.*[165] | 100 m/min | 0.12 mm/rev | Drilling temp. measured<br>Maximum = 79.57 °C<br>Minimum = 38.79 °C |
| Sorrentino *et al.*[160] | 47.1, 251.2, 376.8 m/min | 0.015, 0.05, 0.10, 0.15, 0.20, 0.30 mm/rev | Tool temp. measured,<br>Maximum = 155 °C for CFRP, 195 °C for GFRP at 251.2 m/min cutting speed and 0.10 mm/rev feed rate |

CFRP- Carbon fibre reinforced polymer, GFRP- Glass fibre reinforced polymer.

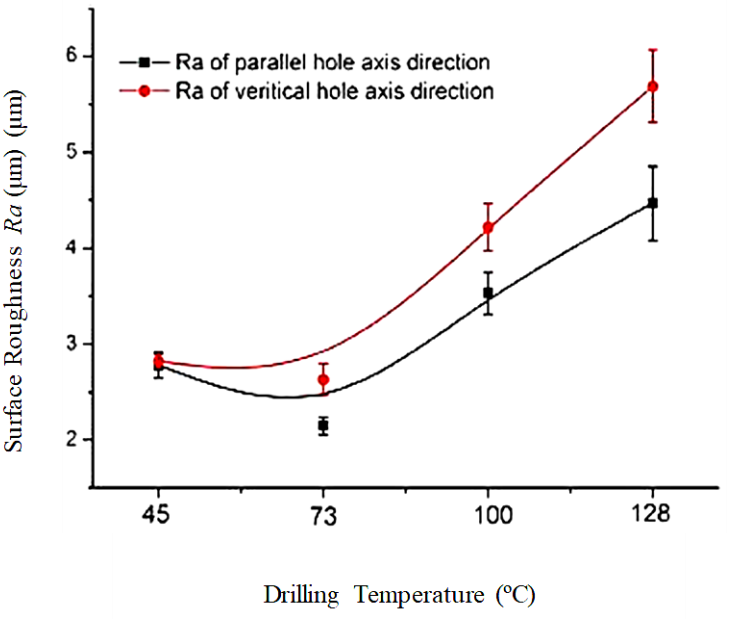


**Fig. 9** Effect of drilling area temperature on surface roughness. Reproduced with the Permission from [88]. Copyright 2018, Springer-Verlag London Ltd.

of 53.8% at 73 °C as shown in below Fig. 9.

Alvarez *et al.*[159] discussed the heat generated during drilling of woven CFRP composite by combining analytical and numerical modeling. The maximum temperature was predicted at the exit of the hole, also initiating mechanical delamination. Similarly, Loja *et al.*[165] confirmed drill geometry and thickness of material displaying more significant influence on maximum temperature-induced whereas, the cutting parameters (spindle speed, feed rate) and material type offered less significance during drilling of GFRP laminates. Moreover, for the same cutting speed and material removal rate, thermal and mechanical load was observed least, in case of orbital drilling compared to the conventional drilling of CFRP. Cracks obtained were perceived at higher cutting speeds during the traditional drilling process, resulting in surface layer damage.[108] Sorrentino *et al.*[160] developed a sensory system for measuring the temperature of the tool and workpiece during the drilling of CFRP and GFRP composites. With decreasing feed rate and increasing cutting speed, the maximum temperature was observed at the tool interface. However, decreasing temperature was noted with an increase in feed rate and cutting speed, whereas for GFRP drilling, the temperature increased with increasing feed rate.

## 5. Recommendations for future work

From the review performed in this article, following are the recommendations proposed for future work:

- More experimental investigation at high temperature and real fire conditions are required for understanding the effect of various factors on fire resistance of FRP composites.
- In comparison to the thermal study of GFRP composites for determining various mechanical properties, limited work has been performed on CFRP composites.
- There is a requirement of more research related to the effect of fibre content and fibre orientation on performance of FRP composites at elevated temperatures.

There is a limited research in enhancing the thermal properties of thermoplastic matrix. Therefore, a further investigation is required by addition of different types of ceramic fillers, fire retardant materials into thermoplastic matrix

## 6. Conclusions

A comprehensive review is presented on mechanical properties (*i.e.* tensile, flexural and compressive) and conventional machining operations (orthogonal cutting, milling, trimming and drilling) subjected to high and low temperature conditions. Based on the studies performed above following conclusions:

- Critical temperature range where 50% strength reduction, noted are, 200 to 300 °C for FRP laminates in tension and 180 to 250 °C in bending.
- High temperature above 300 °C exposure leads to matrix decomposition, limiting the use of composite. Also, in case of cryogenic treatment (*i.e.* -169 to -269 °C), crack initiation takes place at quicker rate due to the contraction of the polymer matrix.
- Epoxy resins are more thermally stable and economical, vinyl ester enhances mechanical properties after post curing, isothalpic-polyester presents lowest mechanical properties instantly with increasing temperature.
- Maximum cutting temperature was obtained for fibre orientation of 90°, for orthogonal cutting and end milling operations.
- The factors significantly influencing the reduced surface

 

roughness in drilling of CFRP composites include low feed rate, high cutting speed, drill geometry and cryogenic air supplied at the interface of tool and composite.

- Cryogenic machining (*i.e.* supplying cool air or liquid nitrogen) is very effective in reducing tool wear and improving the machining surface quality of FRP composites.

## Conflict of interest

There are no conflicts to declare.

## Supporting information

Not applicable.

## References


[1] C. Soutis, *Mater. Sci. Eng. A*, 2005, **412**, 171–176, doi: 10.1016/j.msea.2005.08.064.

[2] K. Friedrich and A. A. Almajid, *Appl. Compos. Mater.*, 2013, **20**, 107–128, doi: 10.1007/s10443-012-9258-7.

[3] M. Guadagnini, *Mech. Compos. Mater.,* 2008*,* **44,** 197–198, doi.org/10.1007/s11029-008-9011-3.

[4] I. Mazinova and P. Florian, *Lect. Notes Mech. Eng.*, 2014, **16**, 145–153, doi: 10.1007/978-3-319-05203-8_21.

[5] B. C. Ray and D. Rathore, *Adv. Colloid Interfac.*, 2014, **209**, 68–83, doi: 10.1016/j.cis.2013.12.014.

[6] S. Dutton, D. Kelly, A. Baker, Composite Materials for Aircraft Structures, American Institute of Aeronautics and Astronautics, Inc. Third Edition, 2016.

[7] D. D. L. Chung, Carbon Fibre Composites, Elsevier Ltd. First Edition, 1994.

[8] H. Dvir, M. Gottlieb, S. Daren, and E. Tartakovsky, *Compos. Sci. Technol.*, 2003, **63**, 1865–1875, doi: 10.1016/s0266-3538(03)00170-2.

[9] S. Wang, D. Haldane, P. Gallagher, T. Liu, R. Liang, and J. H. Koo, *Compos. Part B Eng.*, 2014, **61**, 172–180, doi: 10.1016/j.compositesb.2014.01.049.

[10] M. T. Barako, V. Gambin, and J. Tice, *Nanotechnology*, 2018, **29**, 154003, doi: 10.1088/1361-6528/aaabe1.

[11] Z. Fang, M. Li, S. Wang, Y. Li, X. Wang, Y. Gu, Q. Liu, J. Tian, and Z. Zhang, *Appl. Compos. Mater.*, 2018, **25**, 1255–1268, doi: 10.1007/s10443-017-9664-y.

[12] K. Dong, K. Liu, Q. Zhang, B. Gu, and B. Sun, *Int. J. Heat Mass Tran.*, 2016, **102**, 501–517, doi: 10.1016/j.ijheatmasstransfer.2016.06.035.

[13] Z. Fang, M. Li, S. Wang, Y. Gu, Y. Li, and Z. Zhang, *Int. J. Heat Mass Tran.*, 2019, **137**, 1103–1111, doi: 10.1016/j.ijheatmasstransfer.2019.04.007.

[14] K. K. Mahato, D. K. Rathore, K. Dutta, and B. C. Ray, *Compos. Commun.*, 2017, **3**, 7–10, doi: 10.1016/j.coco.2016.11.001.

[15] D. Kumlutaş, I. H. Tavman, and M. Turhan Çoban, *Compos. Sci. Technol.*, 2003, **63**, 113–117, doi: 10.1016/s0266-3538(02)00194-x.

[16] Y. Le Bozec, S. Kaang, P. J. Hine, and I. M. Ward, *Compos. Sci. Technol.*, 2000, **60**, 333–344, doi: 10.1016/s0266-3538(99)00129-3.

[17] S. Sethi, D. K. Rathore, and B. C. Ray, *Mater. Des.*, 2015, **65**, 617–626, doi: 10.1016/j.matdes.2014.09.053.

[18] M. M. Shokrieh, and M. J. Omidi, *Compos. Struct.*, 2009, **88**, 595–601, doi: 10.1016/j.compstruct.2008.06.012.

[19] B. C. Ray, *Mater. Lett.*, 2004, **58**, 2175–2177, doi: 10.1016/j.matlet.2004.01.035.

[20] B. C. Ray, *J. Reinf. Plast. Compos.*, 2005, **24**, 713–717, doi: 10.1177/0731684405046081.

[21] C. A. Mahieux, and K. L. Reifsnider, *J. Mater. Sci.*, 2002, **37**, 911–920, doi: 10.1023/a:1014383427444.

[22] F. Micelli, and A. Nanni, *Constr. Build. Mater.*, 2004, **18**, 491–503, doi: 10.1016/j.conbuildmat.2004.04.012

[23] M. Bazli, X.-L. Zhao, Y. Bai, R. K. S. Raman, S. Al-Saadi, and A. Haque, *Constr. Build. Mater.*, 2020, **245**, 118399, doi: 10.1016/j.conbuildmat.2020.118399

[24] M. Bazli, H. Ashrafi, and A. V. Oskouei, *Constr. Build. Mater.*, 2017, **148**, 429–443, doi: 10.1016/j.conbuildmat.2017.05.046

[25] A. Jafari, M. Bazli, H. Ashrafi, A. V. Oskouei, S. Azhari X.-L. Zhao and H. Gholipour, *Constr. Build. Mater.*, 2019, **202**, 189–207, doi: 10.1016/j.conbuildmat.2019.01.003

[26] M. Bazli, X.-L. Zhao, Y. Bai, R. K. S. Raman, and S. Al-Saadi, *Eng. Struct.*, 2019, **197**, 109421, doi: 10.1016/j.engstruct.2019.109421

[27] J. R. Cromwell, K. A. Harries, and B. M. Shahrooz, *Constr. Build. Mater.*, 2011, **25**, 2528–2539, doi: 10.1016/j.conbuildmat.2010.11.096

[28] V. K. R. Kodur, L. A. Bisby, and S. H. C. Foo, *ACI Struct. J.*, 2005, **102**, 799.

[29] A. P. Mouritz, and A. G. Gibson, Fire properties of polymer composite materials, Springer Science & Business Media. First Edition, 2007.

[30] R. J. A. Hamad, M. A. M. Johari, and R. H. Haddad, *Constr. Build. Mater.*, 2017, **142**, 521–535, doi: 10.1016/j.conbuildmat.2017.03.113

[31] Y. C. Wang, P. M. H. Wong, and V. Kodur, *Compos. Struct.*, 2007, **80**, 131–140, doi: 10.1016/j.compstruct.2006.04.069

[32] L. A. Bisby, M. F. Green, and V. K. R. Kodur, *Prog. Struct. Eng. Mater.*, 2005, **7**, 136–149.

[33] Y. Bai, T. Vallée, and T. Keller, *Compos. Sci. Technol.*, 2008, **68**, 47–56, doi: 10.1016/j.compscitech.2007.05.039.

[34] Y. C. Wang, and V. Kodur, *Cem. Concr. Compos.*, 2005, **27**, 864–874, doi: 10.1016/j.cemconcomp.2005.03.012.

[35] F. Fleischhaker, A. P. Haehnel, A. M. Misske, M. Blanchot, S. Haremza, and C. Barner-Kowollik, *Macromol. Chem. Phys.*, 2014, **215**, 1192–1200, doi: 10.1002/macp.201400062.

[36] K. H. Tan, and Y. Zhou, *J. Compos. Constr.*, 2011, **15**, 304–311, doi: 10.1061/(ASCE)CC.1943-5614.0000154.

[37] A. Ahmed, and V. K. R. Kodur, *Compos. Part B Eng.*, 2011, **42**, 226–237, doi: 10.1016/j.compositesb.2010.11.004.

[38] M. Leone, S. Matthys, and M. A. Aiello, *Compos. Part B Eng.*, 2009, **40**, 85–93, doi: 10.1016/j.compositesb.2008.06.004.

[39] J. P. Firmo, J. R. Correia, D. Pitta, C. Tiago, and M. R. T.

Arruda, *Cem. Concr. Compos.*, 2015, **60**, 44–54, doi: 10.1016/j.cemconcomp.2015.02.008.
[40] B. Williams, V. Kodur, M. F. Green, and L. Bisby, *ACI Struct. J.*, 2008, **105**, 60.
[41] B. Yu, and V. K. R. Kodur, *Compos. Struct.*, 2014, **110**, 88–97, doi: 10.1016/j.compstruct.2013.11.021.
[42] V. K. R. Kodur, and L. A. Bisby, *J. Struct. Eng.*, 2005, **131**, 34–43, doi: 10.1061/(ASCE)0733-9445(2005)131:1(34).
[43] H. Hajiloo, M. F. Green, M. Noël, N. Bénichou, and M. Sultan, *Compos. Struct.*, 2017, **179**, 705–719, doi:10.1016/j.compstruct.2017.07.060.
[44] X. L. Wang, and X. X. Zha, *App. Mech. And Mater.*, 2011, **71**, 3591-3594, doi: 10.4028/www.scientific.net/AMM.71-78.3591.
[45] M. Saafi, *Compos. Struct.*, 2002, **58**, 11–20, doi:10.1016/S0263-8223(02)00045-4.
[46] Z. Lu G. Xian, and H. Li, *Constr. Build. Mater.*, 2016, **127**, 1029–1036, doi: 10.1016/j.conbuildmat.2015.10.207.
[47] K. Wang, B. Young, and S. T. Smith, *Eng. Struct.*, 2011, **33**, 2154–2161, doi: 10.1016/j.engstruct.2011.03.006.
[48] M. Bazli, and M. Abolfazli, *Polymers (Basel).*, 2020, **12**, 2600, doi: 10.3390/polym12112600.
[49] Graphite, Carbon, *http://www.matweb.com/search/DataSheet.aspx?MatGUID=3f64b985402445c0a5af911135909344&ckck=1*.
[50] Overview of materials for Epoxy, Cast, Unreinforced, *http://www.matweb.com/search/DataSheet.aspx?MatGUID=1c74545c91874b13a3e44f400cedfe39*.
[51] J. F. Timmerman, B. S. Hayes, and J. C. Seferis, *Compos. Sci. Technol.*, 2002, **62**, 1249–1258, doi: 10.1016/s0266-3538(02)00063-5.
[52] V. T. Bechel, J. D. Camping, and R. Y. Kim, *Compos. Part B Eng.*, 2005, **36**, 171–182, doi: 10.1016/j.compositesb.2004.03.001.
[53] P. K. Dutta, and D. Hui, *Compos. Part B Eng.*, 1996, **27**, 371–379, doi: 10.1016/1359-8368(96)00007-8.
[54] J. B. Schutz, *Cryogenics (Guildf).*, 1998, **38**, 3–12, doi: 10.1016/s0011-2275(97)00102-1.
[55] S. Sethi, and B. C. Ray, Polymers at Cryogenic Temperatures, Springer, Berlin, Heidelberg, 2013, 59–113, doi: 10.1007/978-3-642-35335-2_4.
[56] M. Jarrah, E. P. Najafabadi, M. H. Khaneghahi, and A. V. Oskouei, *Constr. Build. Mater.*, 2018, **190**, 38–52. doi: 10.1016/j.conbuildmat.2018.09.086.
[57] S. Cao, W. U. Zhis, and X. Wang, *J. Compos. Mater.*, 2009, **43**, 315–330, doi: 10.1177%2F0021998308099224.
[58] A. G. Gibson, M. E. O. Torres, T. N. A. Browne, S. Feih, and A. P. Mouritz, *Compos. Part A*, 2010, **41**, 1219–1231, doi: 10.1016/j.compositesa.2010.05.004.
[59] S. Kumarasamy, M. S. Z. Abidin, M. N. A. Bakar, M. S. Nazida, Z. Mustafa, and A. Anjang, *IOP Conf. Series: Mater. Sci. and Eng.*, 2018, **370**, 12021, doi: 10.1088/1757-899X/370/1/012021.
[60] R. A. Hawileh, J. A. Abdalla, S. S. Hasan, M. B. Ziyada, and A. Abu-Obeidah, *Constr. Build. Mater.*, 2016, **114**, 364–373, doi: 10.1016/j.conbuildmat.2016.03.175.
[61] S. K. Foster, and L. A. Bisby, 'Proceedings of the 7th International Symposium on Fiber Reinforced Polymer Reinforcement for Reinforced Concrete Structures (FRPRCS-7) ACI SP230-70, 2005, **7**, 1235.
[62] Z. Wu, K. Iwashita, S. Yagashiro, T. Ishikawa, and Y. Hamaguchi, *Zair. Soc. Mater. Sci. Japan*, 2005, **54**, 474–480, doi: 10.2472/jsms.54.474.
[63] J. J. Sha, J. X. Dai, J. Li, Z. Q. Wei, J. M. Hausherr, and W. Krenkel, *Appl. Surf. Sci.*, 2013, **274**, 89–94, doi: 10.1016/j.apsusc.2013.02.102.
[64] A. G. Gibson, T. Browne, S. Feih, and A. P. Mouritz, *J. Compos. Mater.*, 2012, **46**, 2005–2022, doi: 10.1177/0021998311429383.
[65] J. M. Park, D. J. Kwon, Z. J. Wang, G. Y. Gu, and K. L. Devries, *Compos. Part A*, 2013, **47**, 156–164, doi: 10.1016/j.compositesa.2012.12.002.
[66] J. M. L. Reis, J. L. V Coelho, A. H. Monteiro, and H. S. da Costa Mattos, *Compos. Part B Eng.*, 2012, **43**, 2041–2046, doi: 10.1016/j.compositesb.2012.02.005.
[67] M. Shekarchi, E. M. Farahani, M. Yekrangnia, and T. Ozbakkaloglu, *Fire Saf. J.*, 2020, **115**, 103178, doi: 10.1016/j.firesaf.2020.103178.
[68] P. L. Nguyen, *Acad. J. of Civ. Eng.*, 2018, **36**, 472–482, doi: org/10.26168/ajce.36.1.104.
[69] P. L. Nguyen, X. H. Vu, and E. Ferrier, *Fire Saf. J.*, 2018, **100**, 103–117, doi: 10.1016/j.firesaf.2018.07.007.
[70] R. A. Hawileh, A. Abu-Obeidah, J. A. Abdalla, and A. Al-Tamimi, *Constr. Build. Mater.*, 2015, **75**, 342–348, doi: 10.1016/j.conbuildmat.2014.11.020.
[71] H. Ashrafi, M. Bazli, A. Jafari, and T. Ozbakkaloglu, *Compos. Struct.*, 2020, **238**, 111971, doi: 10.1016/j.compstruct.2020.111971.
[72] S. Cao, X. Wang, and Z. Wu, *J. Reinf. Plast. Compos.*, 2011, **30**, 799–807, doi: 10.1177/0731684411411002.
[73] F. Aydin, *Constr. Build. Mater.*, 2016, **127**, 843–849, doi: 10.1016/j.conbuildmat.2016.09.130.
[74] E. U. Chowdhury, R. Eedson, L. A. Bisby, M. F. Green, and N. Benichou, *Fire Technol.*, 2011, **47**, 1063–1080, doi: 10.1007/s10694-009-0116-6.
[75] B. Yu, and V. Kodur, *Compos. Part B Eng.*, 2014, **58**, 510–517, doi: 10.1016/j.compositesb.2013.10.055.
[76] A. G. Gibson, Y.-S. Wu, J. T. Evans, and A. P. Mouritz, *J. Compos. Mater.*, 2006, **40**, 639–658, doi: 10.1177/0021998305055543.
[77] W. Ningyun, and J. T. Evans, *Composites*, 1995, **26**, 56–61, doi: 10.1016/0010-4361(94)P3630-J.
[78] P. S. C. Vieira, F. S. de Souza, D. C. T. Cardoso, J. D. Vieira, and F. de Andrade Silva, *Compos. Part B Eng.*, 2020, **200**, 108335, doi: 10.1016/j.compositesb.2020.108335.
[79] D. G. Schmidt, and J. R. M. d'Almeida, *Fire Technol.*, 2018, **54**, 1565–1583, doi: doi.org/10.1007/s10694-018-0754-7.
[80] T. Aoki, T. Ishikawa, H. Kumazawa, and Y. Morino, in '41st Structures, Structural Dynamics, and Materials Conference and Exhibit', 2000, p. 1605.

 

[81] M. Surendra Kumar, N. Sharma, and B. C. Ray, *J. Reinf. Plast. Compos.*, 2008, **27**, 937–944, doi: 10.1177/0731684407085877.
[82] M. Surendra Kumar, N. Sharma, and B. C. Ray, *J. Reinf. Plast. Compos.*, 2009, **28**, 2013–2023, doi: 10.1177/0731684408090717.
[83] M. Surendra Kumar, N. Chawla, A. Priyadarsini, I. Mishra, and B. C. Ray, *J. Reinf. Plast. Compos.*, 2007, **26**, 1083–1089, doi: 10.1177/0731684407079353.
[84] B. Wang, B. Yang, M. Wang, Y. Zheng, X. Hong, and F. Zhang, *IEEE J. Sel. Top. Quantum Electron.*, 2019, **26**, 394–401, doi: 10.1515/secm-2019-0019.
[85] N. Li, Y. Li, J. Zhou, Y. He, and X. Hao, *Int. J. Mach. Tools Manuf.*, 2015, **97**, 11–17, doi: 10.1016/j.ijmachtools.2015.06.005.
[86] M. Bazli, H. Ashrafi, A. Jafari, X.-L. Zhao, H. Gholipour, and A. V. Oskouei, *Compos. Part B Eng.*, 2019, **157**, 76–99, doi: 10.1016/j.compositesb.2018.08.054.
[87] A. Manalo, S. Surendar, G. van Erp, and B. Benmokrane, *Compos. Struct.*, 2016, **152**, 96–105, doi: 10.1016/j.compstruct.2016.05.028.
[88] H. Wang, X. Zhang, and Y. Duan, *Int. J. Adv. Manuf. Technol.*, 2018, **96**, 2943–2951, doi: 10.1007/s00170-018-1810-7, doi: 10.1007/s00170-018-1810-7.
[89] R. J. Asaro, B. Lattimer, and W. Ramroth, *Compos. Struct.*, 2009, **87**, 382–393, doi: 10.1016/j.compstruct.2008.02.018.
[90] S. Feih, Z. Mathys, A. G. Gibson, and A. P. Mouritz, *Compos. Part A*, 2007, **38**, 2354–2365, doi: 10.1016/j.compositesa.2007.04.013.
[91] C. R. Dandekar, and Y. C. Shin, *Int. J. Mach. Tools Manuf.*, 2012, **57**, 102–121, doi: 10.1016/j.ijmachtools.2012.01.006.
[92] B. K. Lambert, and T. D. Lambert, *Tech. Pap. - Soc. Manuf. Eng. EM*, 1977, **51**, 611–634.
[93] R. V. Rao, and O. P. Gandhi, *J. Inst. Eng. (India), Part PR Prod. Eng. Div.*, 2001, **81**, 52–55.
[94] D. E. Brehl, and T. A. Dow, *Precis. Eng.*, 2008, **32**, 153–172, doi: 10.1016/j.precisioneng.2007.08.003.
[95] R. S. Joshi, and H. Singh, *Mach. Sci. Technol.*, 2014, **18**, 99–119, doi: 10.1080/10910344.2014.863647.
[96] V. Ostasevicius, R. Gaidys, R. Dauksevicius, and S. Mikuckyte, *Stroj. Vestnik/Journal Mech. Eng.*, 2013, **59**, 351–357, doi: 10.5545/sv-jme.2012.856.
[97] J. Du Kim, and E. S. Lee, *J. Mater. Process. Tech.*, 1994, **43**, 259–277, doi: 10.1016/0924-0136(94)90025-6.
[98] Z. W. Zhong, and G. Lin, *Mater. Manuf. Process.*, 2005, **20**, 727–735, doi: 10.1081/amp-200055124.
[99] H. Weber, J. Herberger, and R. Pilz, *CIRP Ann. - Manuf. Technol.*, 1984, **33**, 85–87, doi: 10.1016/s0007-8506(07)61385-7.
[100] J. B. Mann, Y. Guo, C. Saldana, W. D. Compton, and S. Chandrasekar, *Tribol. Int.*, 2011, **44**, 1225–1235, doi: 10.1016/j.triboint.2011.05.023.
[101] K. Debnath, and I. Singh, *J. Manuf. Process.*, 2017, **25**, 262–273, doi: 10.1016/j.jmapro.2016.12.009.
[102] Y. Wang, L. J. Yang, and N. J. Wang, *J. Mater. Process. Technol.*, 2002, **129**, 268–272, doi: 10.1016/s0924-0136(02)00616-7.
[103] G. Chryssolouris, N. Anifantis, and S. Karagiannis, *J. Manuf. Sci. Eng. Trans. ASME*, 1997, **119**, 766–769, doi: 10.1115/1.2836822.
[104] A. Sadek, M. H. Attia, M. Meshreki, and B. Shi, *CIRP Ann. -Manuf. Technol.*, 2013, **62**, 91–94, doi: 10.1016/j.cirp.2013.03.097.
[105] O. Pecat, and E. Brinksmeier, *Procedia CIRP*, 2014, **14**, 142–147, doi: 10.1016/j.procir.2014.03.050.
[106] C. Li, J. Xu, M. Chen, Q. An, M. El Mansori, and F. Ren, *Wear*, 2019, **426–427**, 1616–1623, doi: 10.1016/j.wear.2019.01.005.
[107] A. Sadek, M. Meshreki, and H. Attia, *ICCM Int. Conf. Compos. Mater.*, 2013, **2013**, 3410–3419.
[108] E. Brinksmeier, S. Fangmann, and R. Rentsch, *CIRP Ann. -Manuf. Technol.*, 2011, **60**, 57–60, doi: 10.1016/j.cirp.2011.03.077.
[109] R. M'Saoubi, D. Axinte, S. L. Soo, C. Nobel, H. Attia, G. Kappmeyer, S. Engin, and W. M. Sim, *CIRP Ann. - Manuf. Technol.*, 2015, **64**, 557–580, doi: 10.1016/j.cirp.2015.05.002.
[110] V. M. Miettinen, K. K. Narva, and P. K. Vallittu, *Biomaterials*, 1999, **20**, 1187–1194, doi: 10.1016/s0142-9612(99)00003-4.
[111] M. Woo, and M. R. Piggott, *J. Compos. Technol. Res.*, 1988, **10**, 20–24, doi: 10.1520/ctr10271j.
[112] C. H. Shen, and G. S. Springer, *J. Compos. Mater.*, 1977, **11**, 250–264, doi: 10.1177/002199837701100301.
[113] T. C. Nguyen, Y. Bai, X. L. Zhao, and R. Al-Mahaidi, *Compos. Struct.*, 2012, **94**, 3563–3573, doi: 10.1016/j.compstruct.2012.05.036.
[114] H. Wang, H. Xie, Z. Hu, D. Wu, and P. Chen, *Polym. Degrad. Stab.*, 2012, **97**, 1755–1761, doi: 10.1016/j.polymdegradstab.2012.06.010.
[115] K. B. Shin, C. G. Kim, C. S. Hong, and H. H. Lee, *Compos. Part B Eng.*, 2000, **31**, 223–235, doi: 10.1016/s1359-8368(99)00073-6.
[116] P. Tranchard, F. Samyn, S. Duquesne, M. Thomas, B. Estebe, J. L. Montes, and S. Bourbigot, *J. Fire Sci.*, 2015, **33**, 247–266, doi: 10.1177/0734904115584093.
[117] K. Devendra, and T. Rangaswamy, *Int. J. Comput. Eng. Res.*, 2012, **25**, 2250–3005.
[118] Z. Tao, L. H. Han, and J. P. Zhuang, *J. Constr. Steel Res.*, 2008, **64**, 37–50, doi: 10.1016/j.jcsr.2007.02.004.
[119] Z. Tao, L. H. Han, and L. L. Wang, *J. Constr. Steel Res.*, 2007, **63**, 1116–1126, doi: 10.1016/j.jcsr.2006.09.007.
[120] M. Yaqub, and C. G. Bailey, *Constr. Build. Mater.*, 2011, **25**, 359–370, doi: 10.1016/j.conbuildmat.2010.06.017.
[121] F. ji Wang, J. wei Yin, J. wei Ma, and B. Niu, *Compos. Struct.*, 2018, **197**, 28–38, doi: 10.1016/j.compstruct.2018.05.040.
[122] A. Chatterjee, *J. Appl. Polym. Sci.*, 2009, **114**, 1417–1425, doi: 10.1002/app.30664.
[123] G. Mullier, and J.F. Chatelain, *Int. J. Mech. Aerosp. Ind. Mechatron. Manuf. Eng*, 2015, **9**, 1509–1516.
[124] M. San Juan, O. Martín, F. J. Santos, J. A. Cabezudo, and A. Sánchez, AIP Conference Proceedings, American Institute Of Physics, 2012, **1431**, 495, doi: 10.1063/1.4707601.

[125] H. Wang, J. Sun, J. Li, L. Lu, and N. Li, *Int. J. Adv. Manuf. Technol.*, 2016, **82**, 1517–1525, doi: 10.1007/s00170-015-7479-2.
[126] D. Herzog, P. Jaeschke, O. Meier, and H. Haferkamp, *Int. J. Mach. Tools Manuf.*, 2008, **48**, 1464–1473, doi: 10.1016/j.ijmachtools.2008.04.007.
[127] M. Haddad, R. Zitoune, H. Bougherara, F. Eyma, and B. Castanie, *Compos. Part B Eng.*, 2014, **57**, 136–143, doi: 10.1016/j.compositesb.2013.09.051.
[128] A. Koplev, A. Lystrup, and T. Vorm, *Composites*, 1983, **14**, 371–376, doi: 10.1016/0010-4361(83)90157-x.
[129] O. Pecat, R. Rentsch, and E. Brinksmeier, *Procedia CIRP*, 2012, **1**, 466–470, doi: 10.1016/j.procir.2012.04.083.
[130] X. M. Wang, and L. C. Zhang, *Int. J. Mach. Tools Manuf.*, 2003, **43**, 1015–1022, doi: 10.1016/s0890-6955(03)00090-7.
[131] C. Santiuste, J. Díaz-Álvarez, X. Soldani, and H. Miguélez, *J. Reinf. Plast. Compos.*, 2014, **33**, 758–766, doi: 10.1177/0731684413515956.
[132] B. Denkena, D. Boehnke, and J. H. Dege, *CIRP J. Manuf. Sci. Technol.*, 2008, **1**, 64–69, doi: 10.1016/j.cirpj.2008.09.009.
[133] H. Sasahara, M. Kawasaki, and M. Tsutsumi, *Nippon Kikai Gakkai Ronbunshu, C Hen/Transactions Japan Soc. Mech. Eng. Part C*, 2003, **69**, 2156–2161, doi: 10.1299/kikaic.69.2156.
[134] R. Iyer, P. Koshy, and E. Ng, *Int. J. Mach. Tools Manuf.*, 2007, **47**, 205–210, doi: 10.1016/j.ijmachtools.2006.04.006.
[135] W. Haiyan, Q. Xuda, L. Hao, and R. Chengzu, *Proc. Inst. Mech. Eng. Part B J. Eng. Manuf.*, 2013, **227**, 62–74, doi: 10.1177/0954405412464328.
[136] H. Wang, X. Qin, C. Ren, and Q. Wang, *Int. J. Adv. Manuf. Technol.*, 2012, **58**, 849–859, doi: 10.1007/s00170-011-3435-y.
[137] N. Rajesh Mathivanan, B. S. Mahesh, and H. Anup Shetty, *Meas. J. Int. Meas. Confed.*, 2016, **91**, 39–45, doi: 10.1016/j.measurement.2016.04.077.
[138]Y. Huang, and S. Y. Liang, *Proc. Inst. Mech. Eng. Part C J. Mech. Eng. Sci.*, 2003, **217**, 1195–1208, doi: 10.1243/095440603771665232.
[139] Y. Huang, and S. Y. Liang, *Mach. Sci. Technol.*, 2005, **9**, 301–323, doi: 10.1080/10910340500196421.
[140] I. Lazoglu, and Y. Altintas, *Int. J. Mach. Tools Manuf.*, 2002, **42**, 1011–1022, doi: 10.1016/s0890-6955(02)00039-1.
[141] X. Cui, J. Zhao, and Z. Pei, *Int. Commun. Heat Mass Transf.*, 2012, **39**, 786–791, doi: 10.1016/j.icheatmasstransfer.2012.05.009.
[142] S. Morkavuk, U. Köklü, M. Bağcı, and L. Gemi, *Compos. Part B Eng.*, 2018, **147**, 1–11, doi: 10.1016/j.compositesb.2018.04.024.
[143] Milling Tool and Method, in Particular for Milling Composite Materials, V. Galota A. Falchero and G. Mancina, Google Patents, 2009.
[144] K. Giasin, S. Ayvar-Soberanis, and A. Hodzic, *J. Clean. Prod.*, 2016, **135**, 533–548, doi: 10.1016/j.jclepro.2016.06.098.
[145] Y. Iskandar, A. Tendolkar, M. H. Attia, P. Hendrick, A. Damir, and C. Diakodimitris, *CIRP Ann. - Manuf. Technol.*, 2014, **63**, 77–80, doi: 10.1016/j.cirp.2014.03.078.
[146] A. Shokrani, V. Dhokia, and S. T. Newman, *Int. J. Mach. Tools Manuf.*, 2012, **57**, 83–101, doi: 10.1016/j.ijmachtools.2012.02.002.
[147] X. Yan, J. Reiner, M. Bacca, Y. Altintas, and R. Vaziri, *Compos. Struct.*, 2019, **220**, 460–472, doi: 10.1016/j.compstruct.2019.03.090.
[148] Q. An, J. Chen, X. Cai, T. Peng, and M. Chen, *J. Reinf. Plast. Compos.*, 2018, **37**, 905–916, doi: 10.1177/0731684418768892.
[149] S. Ghafarizadeh, G. Lebrun, and J. F. Chatelain, *J. Compos. Mater.*, 2016, **50**, 1059–1071, doi: 10.1177/0021998315587131.
[150] T. Yashiro, T. Ogawa, and H. Sasahara, *Int. J. Mach. Tools Manuf.*, 2013, **70**, 63–69, doi: 10.1016/j.ijmachtools.2013.03.009.
[151] J. Liu, G. Chen, C. Ji, X. Qin, H. Li, and C. Ren, *Int. J. Mach. Tools Manuf.*, 2014, **86**, 89–103, doi: 10.1016/j.ijmachtools.2014.06.008.
[152] K. Kerrigan, J. Thil, R. Hewison, and G. E. O'Donnell, *Procedia CIRP*, 2012, **1**, 449–454, doi: 10.1016/j.procir.2012.04.080.
[153] M. K. Nor Khairusshima, C. H. Che Hassan, A. G. Jaharah, A. K. M. Amin, and A. N. Md Idriss, *Wear*, 2013, **302**, 1113–1123, doi: 10.1016/j.wear.2013.01.043.
[154] Z. Jia, R. Fu, F. Wang, B. Qian, and C. He, *Polym. Compos.*, 2018, **39**, 437–447, doi: 10.1002/pc.23954.
[155] C. Gao, J. Xiao, J. Xu, and Y. Ke, *Int. J. Adv. Manuf. Technol.*, 2016, **83**, 1113–1125, doi: 10.1007/s00170-015-7592-2.
[156] S. Joshi, K. Rawat, and A. S. S. Balan, *J. Mater. Process. Technol.*, 2018, **262**, 521–531, doi: 10.1016/j.jmatprotec.2018.07.026.
[157] S. Thirumalai Kumaran, T. J. Ko, C. Li, Z. Yu, and M. Uthayakumar, *J. Alloys Compd.*, 2017, **698**, 984–993, doi: 10.1016/j.jallcom.2016.12.275.
[158] J. L. Merino-Pérez, R. Royer, S. Ayvar-Soberanis, E. Merson, and A. Hodzic, *Compos. Struct.*, 2015, **123**, 161–168, doi: 10.1016/j.compstruct.2014.12.033.
[159] J. Díaz-Álvarez, A. Olmedo, C. Santiuste, and M. H. Miguélez, *Materials (Basel).*, 2014, **7**, 4442–4454, doi: 10.3390/ma7064442.
[160] L. Sorrentino, S. Turchetta, and C. Bellini, *Compos. Struct.*, 2017, **168**, 549–561, doi: 10.1016/j.compstruct.2017.02.079.
[161] M. Saleem, L. Toubal, R. Zitoune, and H. Bougherara, *Compos. Part A*, 2013, **55**, 169–177, doi: 10.1016/j.compositesa.2013.09.002.
[162] A. Nagaraj, A. Uysal, and I. S. Jawahir, *Procedia Manuf.*, 2020, **43**, 551–558, doi: https://doi.org/10.1016/j.promfg.2020.02.165.
[163] M. Ferreira Batista, I. Basso, F. Toti, A. Roger Rodrigues, and J. Ricardo Tarpani, *Compos. Struct.*, 2020, 112625, doi: https://doi.org/10.1016/j.compstruct.2020.112625.
[164] W. Ben, G. Hang, W. Quan, W. Maoqing, and Z. Songpeng, *Mater. Manuf. Process.*, 2012, **27**, 968–972, doi: 10.1080/10426914.2011.610079.
[165] M. A. R. Loja, M. S. F. Alves, I. M. F. Bragança, R. S. B. Rosa, I. C. J. Barbosa, and J. I. Barbosa, *Compos. Struct.*, 2018, **202**, 413–423, doi: 10.1016/j.compstruct.2018.02.046.

 

[166] J. Sheikh-Ahmad, F. Almaskari, and F. Hafeez, *Procedia CIRP*, 2020, **85**, 19–24, doi: 10.1016/j.procir.2019.09.048.
[167] G. Caprino, and V. Tagliaferri, *Int. J. Mach. Tools Manuf.*, 1995, **35**, 817–829, doi: 10.1016/0890-6955(94)00055-o.
[168] F. Girot, F. Dau, and M. E. Gutierrez-Orrantia, *J. Mater. Process. Technol.*, 2017, **240**, 332–343, doi: 10.1016/j.jmatprotec.2016.10.007.
[169] N. Shetty, S. M. Shahabaz, S. S. Sharma and S. Divakara Shetty, *Compos. Struct.,* 2017, **176**, 796-802, doi: 10.1016/j.compstruct.2017.06.012.
[170] S. M. Shahabaz, N. Shetty, S. D. Shetty and S. S. Sharma, *Mater. Res. Express*, 2020, **7**, doi: 10.1088/2053-1591/ab6198.
[171] A. P. Singh, and M. Sharma, *Procedia Eng.*, 2013, **51**, 630–636, doi: 10.1016/j.proeng.2013.01.089.
[172] H. Hocheng, and C. C. Tsao, *Int. J. Mach. Tools Manuf.*, 2006, **46**, 1403–1416, doi: 10.1016/j.ijmachtools.2005.10.004.
[173] H. Hocheng, and C. C. Tsao, *J. Mater. Process. Technol.*, 2005, **167**, 251–264, doi: 10.1016/j.jmatprotec.2005.06.039.
[174] C. C. Tsao, K. L. Kuo, and I. C. Hsu, *Int. J. Adv. Manuf. Technol.*, 2012, **59**, 617–622, doi: 10.1007/s00170-011-3532-y.
[175] H. Ho-Cheng, and C. K. H. Dharan, *J. Manuf. Sci. Eng. Trans. ASME*, 1990, **112**, 236–239, doi: 10.1115/1.2899580.
[176] L. Sorrentino, S. Turchetta, and C. Bellini, *Compos. Struct.*, 2018, **186**, 154–164, doi: 10.1016/j.compstruct.2017.12.005.
[177] U. A. Khashaba, Composite Structures, The Military Technical College, 2004, **63**, 313, doi: 10.1016/s0263-8223(03)00180-6.
[178] J. Campos Rubio, A. M. Abrao, P. E. Faria, A. E. Correia, and J. P. Davim, *Int. J. Mach. Tools Manuf.*, 2008, **48**, 715–720, doi: 10.1016/j.ijmachtools.2007.10.015.
[179] J. Y. Sheikh-Ahmad, 'Machining of polymer composites', *Springer*, 2009, doi: 10.1007/978-0-387-68619-6.
[180] D. Kumar, and K. K. Sing, *Mater. Today Proc.*, 2017, **4**, 7618–7627, doi: 10.1016/j.matpr.2017.07.095.
[181] V. Schulze, C. Becke, K. Weidenmann, and S. Dietrich, *J. Mater. Process. Technol.*, 2011, **211**, 329–338, doi: 10.1016/j.jmatprotec.2010.10.004.
[182] V. Krishnaraj, A. Prabukarthi, A. Ramanathan, N. Elanghovan, M. S. Kumar, R. Zitoune, and J. P. Davim, *Compos. Part B Eng.*, 2012, **43**, 1791–1799, doi: 10.1016/j.compositesb.2012.01.007.
[183] N. Feito, J. Díaz-Álvarez, J. López-Puente, and M. H. Miguelez, *Compos. Struct.*, 2018, **184**, 1147–1155, doi: 10.1016/j.compstruct.2017.10.061.
[184] U. A. Khashaba, *J. Compos. Mater.*, 2013, **47**, 1817–1832, doi: 10.1177/0021998312451609.
[185] H. Heidary, N. Z. Karimi, and G. Minak, *Compos. Struct.*, 2018, **201**, 112–120, doi: 10.1016/j.compstruct.2018.06.041.
[186] J. P. Davim, and P. Reis, *Compos. Struct.*, 2003, **59**, 481–487, doi: 10.1016/s0263-8223(02)00257-x.
[187] U. Heisel, and T. Pfeifroth, *Procedia CIRP*, 2012, **1**, 471–476, doi: 10.1016/j.procir.2012.04.084.
[188] R. Q. Sardiñas, P. Reis, and J. P. Davim, *Compos. Sci. Technol.*, 2006, **66**, 3083–3088, doi: 10.1016/j.compscitech.2006.05.003.
[189] M. S. Won, and C. K. H. Dharan, *J. Manuf. Sci. Eng. Trans. ASME*, 2002, **124**, 242–247, doi: 10.1115/1.1448317.
[190] L. Liu, C. Qi, F. Wu, F. Yu, and X. Zhu, *Int. J. Adv. Manuf. Technol.*, 2017, **93**, 953–965, doi: 10.1007/s00170-017-0534-4.
[191] D. F. Liu, Y. J. Tang, and W. L. Cong, *Compos. Struct.*, 2012, **94**, 1265–1279, doi: 10.1016/j.compstruct.2011.11.024.
[192] B. Ramesh, A. Elayaperumal, and S. S. Kumar, *Int. Conf. Mech. Ind. Eng.*, 2013, **3**, 31–36.
[193] B. Ramesh, A. Elayaperumal, A. Joeprasad, and R. R. Ramnath, *Int. J. Sci. Eng. Appl.*, 2012, **1**, 120–126.
[194] P. Mayuet, A. Gallo, A. Portal, P. Arroyo, M. Alvarez, and M. Marcos, *Procedia Eng.*, 2013, **63**, 743–751, doi: 10.1016/j.proeng.2013.08.249.
[195] M. F. Ameur, M. Habak, M. Kenane, H. Aouici, and M. Cheikh, *Int. J. Adv. Manuf. Technol.*, 2017, **88**, 2557–2571, doi: 10.1007/s00170-016-8967-8.
[196] K. Kerrigan, and R. J. Scaife, *Procedia CIRP*, 2018, **77**, 315–319, doi: 10.1016/j.procir.2018.09.024.
[197] F. Impero, M. Dix, A. Squillace, U. Prisco, B. Palumbo, and F. Tagliaferri, *Mater. Manuf. Process.*, 2018, **33**, 1354–1360, doi: 10.1080/10426914.2018.1453162.
[198] G. Basmaci, A. S. Yoruk, U. Koklu, and S. Morkavuk, *Appl. Sci.*, 2017, **7**, 667, doi: 10.3390/app7070667.
[199] T. Xia, Y. Kaynak, C. Arvin, and I. S. Jawahir, *Int. J. Adv. Manuf. Technol.*, 2016, **82**, 605–616, doi: 10.1007/s00170-015-7284-y.
[200] A. Sadek, B. Shi, M. Meshreki, J. Duquesne, and M. H. Attia, *CIRP Ann. -Manuf. Technol.*, 2015, **64**, 89–92, doi: 10.1016/j.cirp.2015.04.074.

## Authors Information

***Mr. S. M. Shahabaz*** *received his bachelor's degree in Mechanical Engineering (Srinivas Institute of Technology, India 2013), Master's degree in Computer Aided Analysis and Design (Manipal University Jaipur, India 2016). He has a teaching experience of 3 years (2016-2019) as an Assistant Professor in the Department of Mechanical Engineering at PA college of Engineering, India. Currently, he is pursuing his Ph. D. in the field of composite materials under the guidance of Dr. Nagaraja Shetty and Dr. Sathyashankara Sharma at Manipal Institute of Technology, India. His area of interest includes 'Study of temperature behavior on mechanical properties and machining of composite materials'. He has published 1 review article and 1 research article in reputed (scopus indexed) journals.*

***Dr. Sathyashankara Sharma*** *holds bachelor's degree in Industrial & Production Engineering (Mysore University, India 1987), Master's degree in Materials Engineering (Mangalore University, India 1996) and PhD degree in Materials Engineering (Manipal*

*University, India 2007). He has 29 years of teaching experience. His area of interest includes Heat Treatment, Deformation of Metals, Material Characterization, Composite Materials. He has published more than 80 (Scopus indexed) research papers in journals and presented more than 50 research papers in conferences.*

***Dr. Nagaraja Shetty*** *received his bachelor's degree in Mechanical Engineering (VTU, India 2007), Master's Degree in Design Engineering (MIT Manipal, India 2010) and PhD degree in Machining of Composite Materials (NIT Karnataka). His area of interest includes Machining of Composite Materials and Manufacturing and Design of Experiments. He is a faculty member at Manipal Institute of Technology, Manipal and carrying his research in the area of Machining of Composite Materials from Manipal University. He has published 41 research papers in journals and presented 15 research papers in international conferences.*

***Dr. Divakara Shetty S*** *received his bachelor's degree in Mechanical Engineering (Mysore University, India 1984), Master's Degree in Engineering Management (MIT Manipal, India 1993) and obtained his Ph. D from Manipal University, in 2007. He has 33 years of teaching experience in MIT Manipal. Presently working as Dean Academic in Mangalore Institute of Technology & Engineering (MITE), Moodabidri, Mangalore. His areas of research include Corrosion Engineering, Personnel Management and Composite materials. He has published 56 research papers in journals and presented 23 research papers in international conferences.*

***Dr. Gowri Shankar M. C*** *received his bachelor's degree in Mechanical Engineering (Mysore University, India 1998), Master's degree in Precision and Quality Eng (IIT Kharagpur, India 2006) and PhD degree in hybrid composites. He has to his credit 7 years of professional experience in industry and more than 15 years in teaching and research. His area of interest includes Manufacturing, Heat treatment and composite materials. He is a faculty member at Manipal Institute of Technology, Manipal and carrying his research in the area of heat treatment and tribology characteristics of composites from Manipal Academy of Higher Education. He has published 55 (Scopus indexed) research papers in journals and presented 15 research papers in international conferences.*



 